Abstract

Enhanced chondrogenic differentiation of adipose-derived stem cells by spheroid culture system

Hee Hun Yoon
School of Chemical and Biological Engineering
The Graduate School
Seoul National University

Damaged articular cartilage has poor intrinsic regenerative capacity, due to its complex and avascular nature. Autologous chondrocyte transplantation (ACT) is a possible treatment, but ACT requires large number of chondrocytes in order to transplant them into the site of defect and the acquisition of choncdocytes relies on *in vitro* expansion of chondrocytes acquired from patient's cartilage. This method involves multiple surgical procedure to harvest and transplant chondocytes, which may cause further cartilage degeneration, and *in vitro* expansion of chondrocytes can result in dedifferentiation of the cells which could diminish the result of the treatment. Current therapeutic approach is cartilage regeneration with usage of mesenchymal stem cells (MSCs) isolated from various adult tissues such as bone marrow and adipose tissue. Among the sources of MSCs, relatively easy harvest method(eg. liposuction) and repeatable

access makes human adipose-derived stem cells (hASCs) an attractive cell source for cartilage regeneration techniques requiring large number of cells.

Generally, one large dense cell aggregate called 'pellet' was made and ,by utilizing this system, chondrogenic differentiation of adult stem cells was induced by supplementing transforming growth factor, dexamethasone, and ascorbate-2-phosphate during culture. But diffusional limitation of nutrients and exertion of heavy hypoxia in the pellet core induces cell death which makes it a unfavorable culture system for chondrogenic differentiation. To enhance the efficacy of chondrogenic differentiation of hASCs, spheroid culture system was evaluated.

In chapter three, hASCs were aggregated into smaller pellet called "spheroid" and spinner flask culture system was implemented to enhance cell-cell interaction and overcome unfavorable factors such as diffusional limitation and enhance chondrogenic differentiation of hASCs. We hypothesized that implementation of spheroid culture system could induce mild hypoxia in the core of the spheroid, which is favorable for chondrogenic differentiation, and enhance interaction between the cells. Both of the factor could result in enhanced chondrogenic differentiation of hASCs. Spheroid is generally induced by a method called "hanging-drop", where cells of certain concentrations are homogeneously suspended and made into droplets which is hanged upside-down. In this study, we implemented spinner flask to induce spheroid, eliminating the conventional method and thus was able to form spheroids with much less time and labour. Formed spheroids were cultured in the spinner flask for 14 days and chondrogenic differentiation was evaluated. *In vitro* chondrogenic differentiation of hASCs was enhanced by spheroid culture compared with monolayer culture. The enhanced chondrogenesis was probably attributable to hypoxia-related cascades and enhanced cell-cell interactions in hASC spheroids. Upon hASCs loading in fibrin gel and transplantation into subcutaneous space

of athymic mice for four weeks, the *in vivo* cartilage formation was enhanced by the transplantation of spheroid-cultured hASCs compared with that of monolayer-cultured hASCs. This study shows that spheroid culture may be an effective method for large scale *in vitro* chondrogenic differentiation of hASCs and subsequent *in vivo* cartilage formation.

In chapter four, we focused on utilizing relatively new material called graphene oxide (GO) to enhance chondrogenic differentiation of hASCs. We hypothesized that presence of the functional groups on GO could interact with extracellular matrix molecules, such as fibronectin (FN) in the culture serum and stably bind growth factors which would help to enhance chondrogenic differentiation of hASCs when interacted with the cell. Using this hypothesis, we interacted GO with the media containing serum and evaluated the proteins absorbed on the GO. GO features both hydrophobic π domains and carboxylic and hydroxyl groups. The π -electron clouds in the GO sheets are capable of interacting with the inner hydrophobic cores of FN and growth factors. It was reported that hydroxyl functional groups stably interact with FN and prevent its deformation. Presence of FN on GO sheets were detected and enhancement of its cellular receptor, integrin expression was detected which could help enhance chondrogenic differentiation. Also, charge-charge interaction of growth factor and GO function groups enabled growth factor absorption onto the GO sheets. FN and growth factor bound GO was than incorporated into spheroids during “hanging-drop” method for even distribution of GO. As formed spheroids were cultured in the spinner culture and the chondrogenic differentiation of hASC spheroids were evaluated.

Keywords: human adipose-derived stem cells, chondrogenic differentiation, spheroid, graphene oxide, tissue engineering

Student Number: 2010-21003

Contents

List of Figures and Table

Chapter 1. Introduction

Chapter 2. Literature review

Chapter 3. Enhanced cartilage formation via three-dimensional cell engineering of human adipose-derived stem cells

Chapter 4. Dual roles of graphene oxide in chondrogenic differentiaton of adult stem cells: cell-adhesion substrate and growth factor-delivery carrier

Chapter 1.

Introduction

1. Introduction

Articular cartilage is a complex, avascular tissue composed of chondrocytes embedded within various extracellular matrices.[1] It covers the articularing surfaces of lone bones in synovial joints and the main function of cartilage is to allow smooth, lower frictional movement of the joints as well as absorbing mechanical forces exerted onto the subchondroal bone.[2] Articular cartilage is sub-classified into elastic, hyaline and fibrocartilage. They differ in the relative amount of major components such as collagen, proteoglycans and elastin fibers.[3] The biochemical properties of cartilage relies on its structure and the composition of the extracellular matrix (ECM).[4] The water content of the ECM is more than 80 % of the total weight of cartilage. Cartilage hydration is crucial for its biomechanical performance such as load bearing joint movement. Chondrocytes are the main cell type of the cartilage. They account for the synthesis and maintenance of the ECM of cartilage.[5] Chondrocytes are seperated from each other by a large amount of ECM. Therefore, nutrient transfer and removal of metabolic waste must occur by diffusion through the ECM.[6] Highly required in our body, unique status of the cartilage limits the intrinsic ability to self-regenerate.

Repair and regeneration of articular cartilage are different processes and need to be classified. Cartilage repair leads to a tissue that is structurally similar to cartilage. However, this repaired tissue does not fully restore the complex structure of the cartilage.[7] Its biochemical composition is more fibrous than hyaline cartilage and its mechanical properties are inferior to that of the latter. Thus, native hyaline cartilage is not re-established in this process.[8] In contrast, cartilage regeneration is defined as the restoration of articular cartilage at the histological, biochemical, and biomechanical levels.[9] Due to a lack of

vascularization in the articular cartilage, access of progenitor cells to the site of a chondral lesion is limited. Thus, chondral defects are in part repopulated by cells that are migrating from the synovial membrane.[10] However, filling of such defects is insufficient and the tissue inevitably degenerates. Furthermore, it integrates poorly with the neighboring cartilage causing discontinuity in the structure.[11] Therefore, these regions become necrotic and in time, it will lead to an increase in the size of the defect. In contrast, osteochondral defect can be filled with a blood clot from the bone marrow through process called 'microfracture'.[11]

Debridement of the lesion and drilling a spacious hole into the bone marrow (microfracture) allows mesenchymal stem cells (MSCs) from the bone marrow to migrate to the site of defect and differentiate into chondrocytes and osteoblasts that later form the cartilaginous repair tissue and the reconstituted subchondral bone, respectively.[12] The process of chondrogenesis is completed after some months and indicated by the appearance of round cells and the presence of a new cartilaginous matrix.[13] However, this repair tissue does not integrate with the existing matrix of the neighbouring cartilage and neighboring articular cartilage do not participate in the filling of the defect but undergo apoptosis over time, and the biomechanical properties of the regenerated cartilage becomes inferior. The new tissue within the defect exhibits a fibrous cartilaginous phenotype and early signs of degeneration. Both, the repair tissue and the cartilage at the periphery of the defect do not withstand mechanical load over time and degenerate after several years.[12] To supplement this technique autologous chondrocyte transplantation (ACT) was developed and it has been clinically practiced since 1987.

ACT is an available treatment for damaged cartilage. Although reports indicate reduced pain and observation of durable cartilage-like tissue after ACT, it requires large number of chondrocytes for transplantation which, therefore,

requires *in vitro* expansion of surgically acquired chondrocytes from the patient. This procedure can further damage the cartilage and the possibility of dedifferentiation of chondrocytes during *in vitro* expansion can cause inadequate regeneration after treatment. Therefore, alternative cell sources were considered.[14]

Application of progenitor cells (eg. MSCs) is an attractive method regeneration improvement in sites of cartilage defect compared to implantation of differentiated cells like chondrocytes.[15] MSCs possesses reliable potential for differentiation into cells of the mesodermal lineage .[16,17] They also have homing, trophic, and immunomodulatory activities[18,19] that may favorably influence the activities of unaffected cells in the neighbouring cartilage upon implantation.

MSCs can be isolated from various tissues including bone marrow[20] and adipose.[21] Since MSCs have adhering property, they can ben expanded and maintain multipotency *in vitro*. During culture, they can be induced to generate chondrocytes and other mesodermal lineages such as osteoblasts and adipocytes.[22] MSCs show promise for repairing and reconstructing damaged mesenchymal tissues. Compared with bone marrow-derived MSCs, adipose-derived MSCs (ASCs) from lipoaspirates are acquired using a less invasive procedure and in abundance.[23] ASCs can commit toward the chondrogenic, osteogenic, adipogenic, myogenic, and neurogenic lineages.[24] ASCs can undergo a higher number of passages before senescence, showing enhanced rates of proliferation.[25]

Previously, *in vitro* chondrogenesis of ASCs were induced in pellet, a large cell aggregate, with supplementation of transforming growth factor (TGF), dexamethasone, and ascorbate 2-phosphate. Growth factors can be used to induce and enhance chondrogenic differentiation.[26] Members of the TGF-β superfamily have been demonstrated to be important in chondrogenic differentiation of expanded chondrocytes.[26] To avoid cartilage donor site morbidity, replicative chondrocyte dedifferentiation during *in vitro* expansion,

attempts were made to stimulate MSCs to differentiate to cartilage during 4 weeks in the presence of cell culture medium containing TGF-β.[27] TGF-β was also used to induce chondrogenic differentiation of progenitor cells derived from sources such as adipose tissue. Although enhanced chondrogenic differentiation was achieved in the pellet system, heavy hypoxic condition within the pellet core, as well as the diffusional limitation of nutrients in the pellet causes cell death.[28] Thus, a alternative method for effective *in vitro* chondrogenic differentiation is in need.

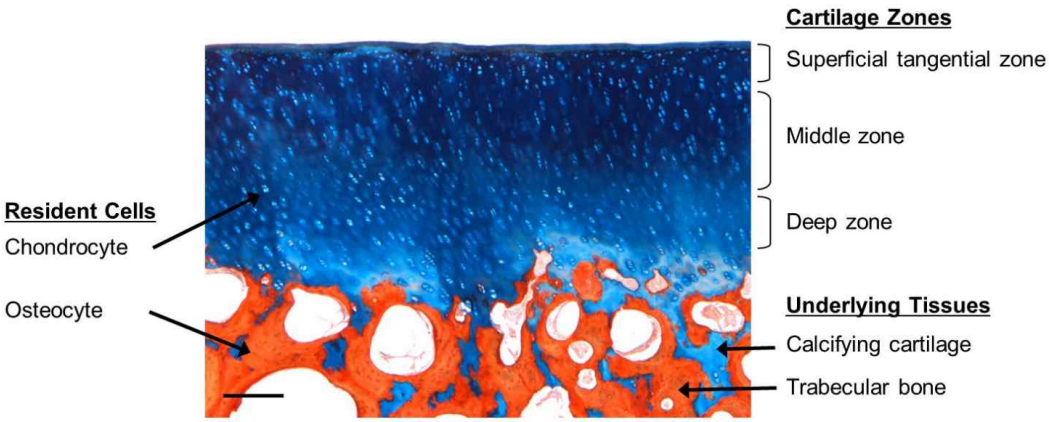

Figure. 1.1. Complex structure of the cartilage. Section of cartilage detailing the various zones.

2. Objectives

In this research, small cell aggregates (hereafter mentioned as spheroids) were applied in *in vitro* chondrogenic differentiation of human ASCs (hASCs) using bioreactor system.

In chapter three, spheroid formation within the bioreactor itself without additional handling was optimized. Briefly, cells were placed in a spinner flask (bioreactor) and allowed to sediment and were stirred at low rpm. Spheroids were formed at day 3 and were culture for 14 days under controlled environment. After 14 days, half of the samples were evaluated for chondrogenic differentiation. Other half was subcutaneous transplanted onto athymic mouse for 28 days and were evaluated for cartilage formation. In this chapter we hypothesized that formation of such spheroid would enhance chondrogenic didfferentiation of hASCs via enhanced cell-cell interaction and induced mild hypoxia. The mechanism of enhanced chondrogenic differentiation was elucidated. Also applicability of sheroid culture system for large scale culture was assessed.

In chapter four, graphene oxide (GO) was evaluated as a material to enhance chondrogenic differentiation of hASCs. We focused to utilize and interact GO's available functional groups with extracellular matrices and growth factors in favor to chondrogenic differentiation and implemented them to spheroid culture system. GO was incorporated after successfully interacting it with fibronectin and transforming growth factor. Spheroids were culture for 14 days and were evaluated for chondrogenic differentiation. Enhanced chondrogenic differentiation of hASCs by GO incorporation was assessed in terms of cell-adhesion substrate providence and growth factor delivery efficacy. From this aspect, GO was evaluated in terms of compatibility with the spheroid culture system developed.

Chapter 2.

Literature review

1. Cartilage

Due to its avascular structure, cartilage tissue has limited innate regenerative ability. In 1743, William Hunter "…when cartilage is destroyed, it is never recovered".[29] Since then, various techniques including marrow stimulation, autologous chondrocyte transplantation (ACT), tissue engineering, and other techniques have been explored to improve cartilage regeneration.[30,31] However, till date, no technique has reliably regenerated the cartilage with full biological and biomechanical properties.

In general, surgical intervention for cartilage lesions can be divided into marrow-stimulating techniques and reconstructive techniques. microfracture is a surgical techniques for bone marrow stimulation, which may stimulate healing by breaking bone around the defect but and stimulating bone marrow flow into the defect but can result in the production of an inferior quality of newly formed fibrocartilage tissue.[31] Reconstructive techniques include ACT and other variations of tissue engineering.[32] ACT involves removal of healthy chondrocytes from a patient and the implantation of these into a defective cartilage site, stimulating the growth of new hyaline cartilage. However, the drawbacks of ACT include limited cell sources, difficulty in phenotype retention, and donor-site morbidity, all of which challenge autologous cell transfer procedures.[33] Thus, new strategies rely upon cell therapies that explore the use of stem cells rather than primary chondrocytes for cartilage regeneration. Since the range of potential cell sources for cartilage regeneration is so extensive, the following criteria may help identify the best candidate cell sources for cartilage regeneration: 1) easy to isolate and collect, 2) easy to expand, 3) can expressing and synthesize cartilage-specific molecules, 4) can produce comparable mechanical properties to native cartilage, 5) can integrate into the

surrounding cartilage, and 6) immunocompatible.[30,34,35]

1.1. Extracellular Matrices of Cartilage

1.1.1. Collagen

Various collagen types are present in articular cartilage and type II collagen takes up 90 - 95% of the collagen proportion. Type II collagen has a high amount of bound carbohydrates which allows more interaction with water. Types IX and XI form a 'mesh' and this structure provides tensile strength. Although not much is known, type IX has been observed to bind to the fibers and extend into the inter-fiber space to interact with other type IX molecules, possibly acting to stabilize the mesh structure. Type X is found only near areas of the matrix that are calcified.[36,37]

1.1.2. Proteoglycans

Proteoglycans consists of 95 % polysaccharide and about 5 % protein. The protein core is associated with various glycosaminoglycan (GAG) chains. GAG chains are unbranched polysaccharides made from disaccharides of an amino sugar and another sugar. At least one component of the disaccharide has a negatively charged sulfate or carboxylate group, so the GAGs tend to repel one another and anions while attracting cations and facilitate interaction with water. Hyaluronic acid, dermatan sulfateare, chondroitin sulfate and keratan sulfate are some of the GAGs found in articular cartilage.[37,38]

1.2. Tissue Fluid

Tissue fluid is an essential part of hyaline cartilage and makes up 80 % of the wet weight of the tissue. Addition to water, the fluid contains metabolites and abundant cations to balance the negatively charged GAGs in the ECM. Exchange of this fluid with the synovial fluid provides necessary resources to the avascular cartilage. In addition, the entrapment of this fluid though interaction with ECM components provides the tissue with its ability to resist compression retain its shape.[37,38]

2. Cell Sources

2.1. Articular Chondrocytes

Mature articular cartilage is organized into superficial, middle, and deep zones. The superficial zone is at the articular surface, whereas the deep zone adjoins the calcified cartilage, which integrates into the subchondral bone. Chondrocytes from different zones have unique gene expression profiles of markers and matrix protein expression levels.[39] Chondrocytes from the deep zone proliferate faster, produce more ECM with a greater amount of glycosaminoglycans compared to other zones. Interestingly, engineered cartilage tissues grown *in vitro* from chondrocytes show different zonal properties corresponding to the zone from which the cells were isolated.[40] However, culture conditions and cell–cell communication affect the retention of zonal-specific characteristics in alginate culture, but not in pellet culture.[41]

Articular chondrocytes have proven to be implementable cell source for surgical operations such as ACT. The most common articular chondrocyte-based

surgical procedure is ACT and it was first applied to a knee cartilage defect in 1994. Since then, it has been widely studied in the field of cartilage regeneration.[42] In the ACT process, autologous articular chondrocytes are collected from a low-load-bearing area of a joint, expanded *in vitro*, resuspended, injected into a defect. Generally, improved healing responses are reported with ACT treatment; neocartilage-like tissue is often formed, and defects are filled more completely with chondrocyte treatment than when left untreated or treated with cell-free therapies. Although the newly formed tissue is mainly fibrocartilaginous, some long-term follow-up studies suggest that the clinical functionality of ACT remains high even 10–20 years after the implantation.[43,44] However, other studies have found the benefit of ACT more questionable. A randomized trial found no histological or clinical difference between microfracture and ACT treatment groups at 2 years after surgery, and the microfracture group showed better results.[45] A more comprehensive review of 9 trials with 626 patients found no advantage of ACT over other treatments.[46] Hence, there is no sufficient existing randomized trial to prove the superiority of ACT to other treatment strategies for full-thickness cartilage defects.

2.2. Bone Marrow-derived Stem Cells (BMSCs)

BMSCs are commonly used in tissue engineering and have been well studied since they can form cartilage-like structures *in vitro* and stimulate cartilage repair *in vivo*. Surgical techniques utilizing BMSCs include pridie drilling and microfracture. These techniques repair fibrocartilage by bone stimulation which is done by drilling small holes into the subchondral bone after debridement of

cartilage defects. They are some of the most frequently used techniques and work by stimulating bone marrow to encourage marrow progenitor cells to migrate to the lesion. BMSCs, growth factors, and cytokines are released into the defect and progenitor cells can differentiate into chondrocytes to begin to form new fibrocartilage or hyaline-like cartilage.[47] These methods have proven safe and effective in many studies, and microfracture was successful in the treatment of full-thickness chondral lesions of the knee.[48] However, a recent report denoted that microfracture works only in the short term, whereas ACT provides prolonged healing.[49] Moreover, bone marrow stimulation often generates fibrocartilage tissue with lower type II collagen content.[50] Since many studies have found surgical fracture techniques unsuccessful at restoring normal hyaline cartilage, studies have begun to explore areas of stem cell-based tissue engineering.[51] BMSCs have been cultured in a various of 3D scaffold systems to generate cartilage-like tissue.[52-56] In general, cartilage-like tissue could be induced using BMSCs regardless of scaffold composition and structure both *in vitro* and *in vivo*. Addition of growth factors like transforming growth factor can enhance chondrogenesis.[57]

A series of clinical ACT studies were conducted where culture-expanded BMSCs were embedded in collagen gels and transplanted into cartilage.[58-62] In 2002, this system was tested on patients with knee osteoarthritis and where 12 of 24 patients were treated with BMSCs whereas the other 12 were served as negative controls. After 42 weeks, the results indicated better arthroscopic and histological scores in the BMSC transplanted group, but no significant clinical improvement was found.[62]

2.3. Adipose-derived Stem Cells (ASCs)

ASCs potential to chondrogenically differentiate has been validated *in vitro* by variety of culture conditions. Type II collagen and aggrecan can be induced in ASCs when maintained in chondrogenic medium and aggrecan protein can be secreted. *In vivo* experiments have verified that ASCs which underwent chondrogenesis can proliferate and form new cartilage after subcutaneous injection with fibrin glue.[63] In an *in vitro* pellet culture, ASCs also showed enhanced chondrogenic differentiation compared with human umbilical cord matrix cells.[64] ASCs resemble BMSCs in their phenotype and their ability to differentiate into several mesenchymal lineages including chondrocyte. Both cell types are recognized as potential cell sources for cartilage repair, but ASCs appears advantageous in a few ways. ASCs can be obtained via less invasive method like liposuction. However, some studies showed that ASCs have inferior chondrogenic potential compared with BMSCs and that pellet cultures of ASCs show much weaker chondrogenesis.[65] However, in *in vivo* studies, conflicting results for cartilage repair by ASCs are reported where ASCs can heal full-thickness cartilage defects and form a hyaline-like cartilage tissue.[66]

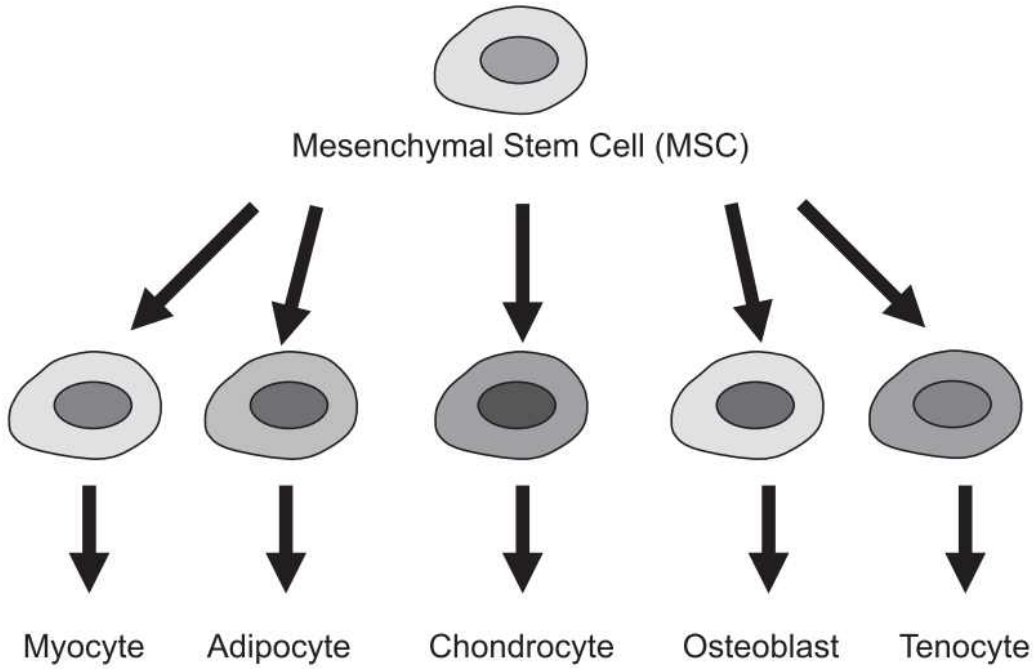

Figure. 2.1. The mesenchymal stem cell (MSC) lineage. MSCs are multipotent stem cells capable differentiating into variety of differentiated cells.

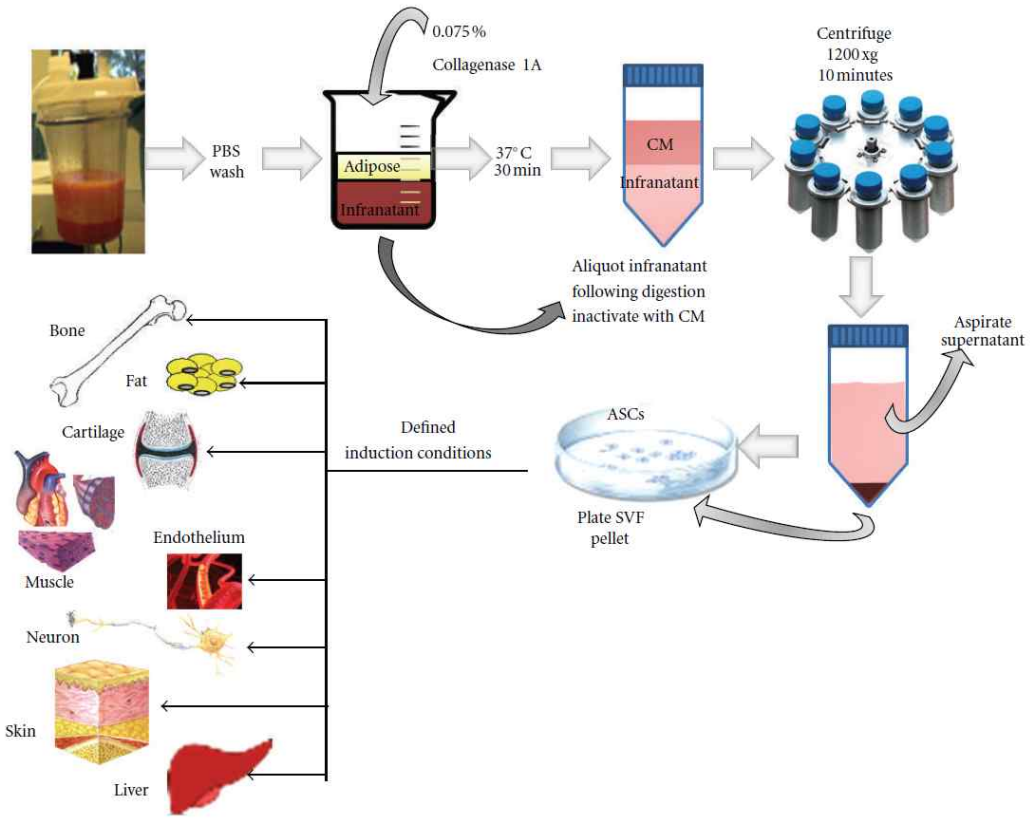

Figure. 2.2. ASC isolation and utilization. Schematic outlline of the isolation of ASCs from lipoaspirates showing the enzymatic digestion of adipose tissue with collagenase type IA and the isolation of the SCF via centrifugation. Plating of the SCF results in eventual selection and expansion of the ASC population. Induction of ASCs under defined conditions can result in their differentiation to multiple cell types.

2. Current Clinical Methods for Cartilage Repair

The main aspect of articular cartilage repair is filling of the defect and restoration of its native tissue structure. Focusing on articular cartilage, two clinical approach can be mentioned; microfracture and autologous chondrocyte transplantation (ACT).

Microfracture, also known as subchondral marrow stimulation, is achieved by drilling and forming cortical penetration. After clearing the defect of the debris, conical holes of 0.5 to 1 mm in diameter are punched over the defect area, each distanced by 3 to 4 mm. Consequently, a blood clot fills he defect followed by ingrowth of bone marrow cells.[67] For favorable result, it is recommended that this technique is to be applied to patients younger than 45 years old, experienced injury related symptoms less than a year, and the defect size should be less than 4 cm^2 in diameter.[68]

Improvements in the symptoms are widely reported up to 2 years but the symptoms are generally expected to return.[69] The histological analysis of the biopsies acquired of these tissues, lesions were found to consist mainly of fibrocartilage rather than hyaline cartilage. This result indicate that bio-functionalities are not equivalent to the native articular cartilage.[70] Augmentation to this techniques are actively being explored.

The inconsistent results of microfracture lead the development of autologous cartilage transplantation (ACT)[71] The principle of ACT is to implant autologous chondrocytes into the cartilage defect in order to fill it with newly synthesized cartilage matrix. The procedure involves surgical step to extract chondrocytes from non-load bearing area of healthy articular cartilage. Chondrocytes are then isolated by collagenase treatment and expanded *in vitro*. During the second surgery, injured cartilage is debrided and the defect is covered with a periosteal

flap, which is taken from the medial tibia. Finally, 50 – 100 µl chondrocyte cell suspension of 2.6 – 5 million cells are injected.[72] With a follow-up period of 2 – 10 years, results of clinical studies revealed well integrated repair tissue in 90 % of treated patients.[73]

ACT has three major drawbacks: need of two operations, a long rehabilitation period, and ACT being a multistage, complicated procedure. The most frequently reported adverse event after ACT is hypertrophy of the periosteal flap used in the procedure.[74] Alternate approaches such as utilization of artificial matrices consisting of mixture of collagens or hyaluronic acid scaffolds has been practiced.[75-77] However, these materials increase the probability of immune reaction, and their use is currently considered off-label in the USA. Preliminary studies have also shown that autologous chondrocytes 'dedifferentiate' into fibrochondrocytes in culture.[78] However, other work shows they can redifferentiate and express chondrocyte-like markers after being reintroduced into a three dimensional *in vitro* culture system.[79] Nevertheless, large-scale cohort studies are needed to further investigate the cost-effectiveness of ACT. Overall, ACT has proven beneficial, but more research is in need to develop biomechanically stable matrices and to achieve faster maturation of the regenerated tissue. Further work is necessary to standardize and optimize the technique and the post-surgery predictions.

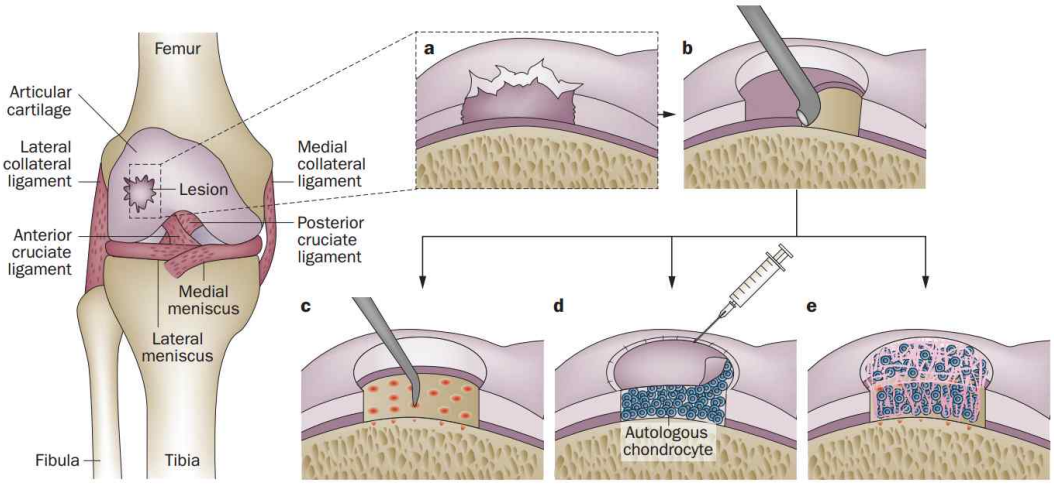

Figure. 2.3. Cartilage regeneration techniques. (a) Full thickness lesion; (b) debribement of the lesion; (c) microfracture; (d) ACT, (e) matrix assisted ACT.

3. Tissue Engineering Approach

In order to assist and / or improve currently available treatments, tissue engineering approaches are extensively being explored. To assist microfracture, artificial matrices are implemented which aims to delivery growth factors and provide cell signalling at the site of lesion. Such growth factors can activate surrounding chondrocytes of the healthy cartilage and help to remodel the repaired tissue.[80] Tissue engineering can be defined as the reconstitution of tissues, both structurally and functionally. Such reconstruction processes can be conducted either entirely *in vitro* or partially *in vitro* and then completed *in vivo*, *in situ*. This technology would eliminate the need for tissue transplantation. If the appropriate cell source could be obtained, problems associated with donor tissue usage would be avoided.

Implanting polymer-based matrix combined with autologous serum or platelet-rich plasma after microfracture has been proposed as a novel *in situ* strategy.[81] Autologous serum and platelet-rich plasma can help to recruit MSCs from subchondral bone.[82] A multi-centered, randomized clinical trial of chitosan-glycerol phosphate and microfracture resulted in superior quality of repair tissue than microfracture alone.[83] The lack of a supportive scaffold material to guide matrix symthesis and organization might account for the outcome of treatments. *Ex vivo* studies showed successful cartilage regeneration is dependent on chondrocyte proliferation and differentiation capacity of stem cells within the tissue. Thus, the second generation of ACT focuses on the development of scaffold-based approaches for delivering chondrocytes to defect site. The major advantages of this technique are better filling of the defect and shorter recovery period. Also cluture of chondrocyte in 3D environment facilitates to prevent dedifferentiation, therefore, produce cartilage with improved

quality.

Another approach is a matrix free transplantation of differentiated stem cells. Without scaffold to interrupt cell-cell signalling, the neotissue microenvironment might be more favorable, which can enhance the response to stimulation and integration with surrounding healthy tissue.[80] Studies found that stimulation of self-assemble artilage cartilage with exogenous stimulation promoted the development of neotissue with similar functional properties as native cartilage.[80,84] These studies also found that scaffold-free neotissue is capable of both integration and *in vivo* maturation. When compared with scaffold-based techniques, the scaffold-free neotissue has superior mechanical properties and a higher percentage of ECM. Another scaffold-free technology for articular cartilage regeneration is based on transplantation of chondrosphere.[85] The clinical efficacy of chondrosphere transplantation is currently under phase III clinical trial in Europe. However, data from this clinical trial are not yet available. Overall, scaffold-free neotissue could facilitate development of highly bioactive implants to enhance cartilage regeneration.

Chapter 3.

Enhanced cartilage formation via three-dimensional cell engineering of human-adipose derived stem cells

1. Introduction

Damaged articular cartilage has poor intrinsic regenerative capacity, due to its avascular nature. Autologous chondrocyte transplantation is a possible treatment, but this procedure requires the isolation of chondrocytes via surgery, which may cause further degeneration of the cartilage.[86] An alternative approach is cartilage regeneration utilizing MSCs isolated from adult tissues such as bone marrow[87] and adipose tissue.[88] hASCs are relatively accessible and attractive as a cell source for cartilage regeneration, due to the simple surgical procedures, that are required to harvest the cells, the repeatable access to the subcutaneous adipose tissue, and relatively easy enzyme-based isolation procedures.[89,90]

Generally, *in vitro* chondrogenic differentiation of ASCs is induced by culturing ASCs in a pellet with the supplementation of transforming growth factor (TGF), dexamethasone, and ascorbate-2-phosphate.[91-93] Winter et al. showed that bone marrow-derived MSCs (BMMSCs) and ASCs showed indistinguishable chondrogenic potential in monolayer culture.[94] However, in pellets or spheroids, BMMSCs showed improved chondrogenesis compared to ASCs.[91,92,94] It was reported that MSC culture in hydrogels of either collagen type II[95] or hyaluronic acid[96] promotes chondrogenesis. Pellet culture is inappropriate for large-scale culture to obtain adequate number of cells for clinical applications, because the pellet culture produces only one pellet in each culture tube. In contrast, cultivation using three-dimensional bioreactors (e.g., spinner flasks) can produce a large number of cell spheroids or pellets and facilitate culture in large scale.[97] Previously, we have developed a spinner flask culture system for efficient formation of ASC spheroids.[98] In this study, the spheroid formation and chondrogenic differentiation of hASCs were induced on a large scale by culturing hASCs in spinner flasks (Figure. 3.1.). The

mechanisms for enhanced chondrogenic differentiation of hASCs cultured in spheroids compared with monolayer culture were also investigated. Additionally, to evaluate the *in vivo* cartilage forming ability of the cells, hASCs cultured either in spheroid form or in monolayer were loaded into fibrin gels and were subcutaneously transplanted into athymic mice for four weeks. Cartilaginous tissue formation was evaluated with histological, immunohistochemical, reverse transcription-polymerase chain reaction (RT-PCR), and western blot analysis.

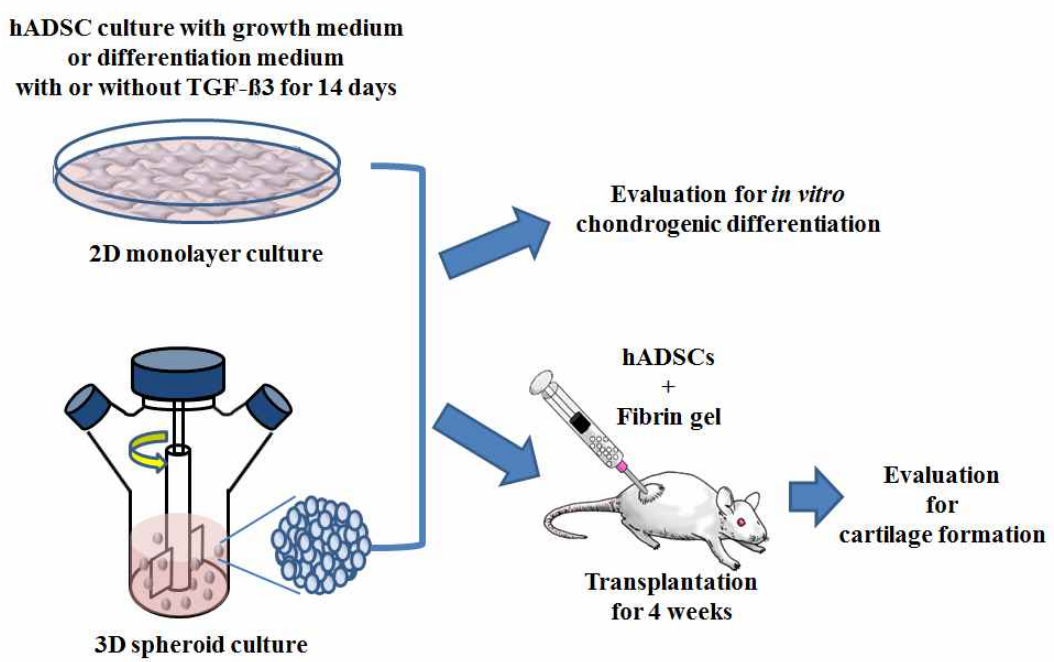

Figure. 3.1. Schematic diagram describing experimental procedure of the present study.

2. Materials and Methods

2.1. The Isolation and Culture of hASCs

The hASCs were isolated from lipoaspirates that were collected from informed and consenting patients, and subsequently cultured, as previously described.[88] The hASCs were cultured in growth medium consisting of α -minimum essential medium (α-MEM, Gibco BRL, Gaithersburg, MD, USA), 10 % (v/v) fetal bovine serum (FBS, Gibco BRL), 100 units/ml of penicillin, and 100 μg/ml of streptomycin. The hASCs at the fourth passage of cultivation were utilized for the experiments in this study

2.2. The Formation and Culture of Spheroids

The ASCs were placed into a spinner flask (working volume = 100 ml, Wheaton, Millville, NJ, USA) at 1.0 x 10^6 cells/ml in differentiation medium consisting of Dulbecco's modified Eagle's medium high glucose (GibcoBRL), 50 mg/ml of ascorbic acid, and 100 nM of dexamethasone supplemented either with or without 10 ng/ml of TGF-β3 (R&D systems, Minneapolis, MN, USA) and stirred at 40 rpm. The spinner flasks were siliconized with sigmacoat (Sigma, St. Louis, MO, USA) to prevent cell adhesion onto the flask walls before use. The spheroids formed on day 3. For medium exchange, the spheroids were allowed to settle, and 80 % of the supernatant was replaced with fresh medium every other day. As a control, hASCs were also cultured in a monolayer with the differentiation medium.

2.3. Scanning Electron Microscope (SEM)

For SEM analysis, the spheroids were washed twice with phosphate-buffered saline (PBS), prefixed with 4% (v/v) buffered glutaraldehyde (Sigma) for 1 h, and were fixed with 0.1% (v/v) buffered formaldehyde (Sigma) for 24 h. The fixed specimens were dehydrated in ascending grades of ethanol, dried, and mounted on aluminum stubs. The specimens were subsequently coated with platinum using a Sputter Coater (Cressington 108, Cressington Scientific Instruments, Cranberry, PA, USA) and examined by SEM (JSM-6330F, JEOL, Tokyo, Japan).

2.4. The Transplantation of the Spheroid-Fibrin Gel Mixture

Monolayer hASCs (3 x 10^6 cells) or hASC spheroids (3 x 10^6 cells) in differentiation medium supplemented with or without TGF-β3 for 14 days were loaded into 60 μl fibrin gels (Greencross, Seoul, Korea) and were transplanted subcutaneously into 4 week old athymic mice (Orient Bio Inc., Sungnam, Korea) (n = 4 transplants per group). The number of monolayer hASCs and spheroid hASCs was determined by quantifying DNA-binding dye Hoechst 33258 dye (Molecular Probes, Eugene, OR, USA). After 28 days, the transplants were removed. The specimens were cut in half and were subjected to analysis by histology, immunohistochemistry, RT-PCR, and western blot. The animal study was approved by the Institutional Animal Care and Use Committee at Seoul National University (#100203-4).

2.5. Histology and Immunohistochemistry

The *in vitro* cultured spheroids were harvested on day 14. The neotissues formed by the hASC transplantation were removed on day 28 after transplantation. The specimens were fixed in 10 % (v/v) buffered formaldehyde, dehydrated in a graded ethanol series, and embedded in paraffin. The specimens were sliced into 4 μm sections. The sections were stained with hematoxylin and eosin (H&E) and alcian blue. The sections were also stained with anti-type II collagen antibodies (Abcam, Cambridge, UK) and counter-stained with 4,6 diamidino-2-phenylindole (DAPI, Vector Laboratories, Burlingame, CA, USA) for immunohistochemical analysis. Next, the immunohistochemical images were examined with a fluorescence microscope (Olympus IX 71, Olympus, Tokyo, Japan).

2.6. RT-PCR Analysis

The cell or tissue samples were lysed with TRIzol reagent (Invitrogen, Carlsbad, CA, USA). The total RNA was extracted with chloroform (Sigma) and precipitated with 80 % (v/v) isopropanol (Sigma). After the supernatant was removed, the RNA pellet was washed with 75 % (v/v) ethanol, air-dried, and dissolved in 0.1 % (v/v) diethyl pyrocarbonate-treated water (Sigma). The RNA concentration was determined by measuring the absorbance at 260 nm with a spectrophotometer. Reverse transcription was performed with 5 μg of pure total RNA and SuperScriptTM II reverse transcriptase (Invitrogen), and was followed by PCR amplification of the synthesized cDNA. The PCR consisted of 35 cycles of denaturing (94 °C, 30 sec), annealing (58 °C, 45 sec), and extension (72 °C, 45 sec), with a final extension at 72 °C for 10 min. The PCR was

followed by electrophoresis on a 2 % (w/v) agarose gel and DNA visualization by ethidium bromide staining. The PCR products were analyzed with a gel-documentation system (Gel Doc 1000, Bio-Rad, Hercules, CA, USA). SOX-9 (S: 5'- CCC AAC GCC ATC TTC AAG G -3', AS: 5'- CTG CTC AGC TCG CCG ATG T -3'), aggrecan (S: 5'- GCC TTG AGC AGT TCA CCT TC -3', AS: 5'- CTC TTC TAC GGG GAC AGC AG -3'), hypoxia inducible factor (HIF)-1α (S: 5'-CCA GTT AGG TTC CTT CGA TCA GT-3', AS: 5'-TTT GAG GAC TTG CGC TTT CA-3'), and TGF-β3 (S: 5'- ACA TTT CTT TCT TGC TGG -3', AS: 5'- GGG GAA GAA CCC ATA ATG -3') were used. β -actin (S: 5'-CCT TCC TGG GCA TGG AGT CCT G-3', AS: 5'-GGA GCA ATG ATC TTG ATC TTC-3') served as the internal control. The amount of RT-PCR results was quantified with an Imaging Densitometer (Bio-Rad).

2.7. Real Time-PCR Analysis

Real-time PCR analysis (n = 3 per group) was performed to quantify the relative gene expression level of type II collagen (S: 5'-ATA AGG ATG TGT GGA AGC CG-3', AS: 5'-TTT CTG TCC CTT TGG TCC TG-3'), SOX-9 (S: 5'-GGA GCT CGA AAC TGA CTG GAA-3', AS: GAG GCG AAT TGG AGA GGA GGA-3'), aggrecan (S: 5'-GCC TTG AGC AGT TCA CCT TC-3', AS: 5'-CTC TTC TAC GGG GAC AGC AG-3‘), and TGF-β3 (S: 5'- ACA TTT CTT TCT TGC TGG -3', AS: 5'- GGG GAA GAA CCC ATA ATG -3‘). The total RNA was extracted from the hASCs after chondrogenic differentiation treatment using 1 ml of TRIzol reagent (Invitrogen, Carlsbad, CA, USA) and 200 μl of chloroform. The hASCs and spheroid lysate samples were centrifuged at 12,000 rpm for 10 min at 4 °C. The RNA pellets were washed with 75 % (v/v) ethanol and dried. After the drying procedure, the samples were dissolved

in RNase-free water. The iQ™ SYBR Green Supermix kit (Bio-Rad Laboratories, Hercules, CA, USA) and the MyiQ™ single color Real-Time PCR Detection System (Bio-Rad Laboratories) were used.

2.8. Western Blot Analysis

The specimens (n = 3 per group) were lysed in ice-cold lysis buffer (15 mM Tris HCl (pH 8.0), 0.25 M sucrose, 15 mM NaCl, 1.5 mM $MgCl_2$, 2.5 mM EDTA, 1mM EGTA, 1mM dithiothreitol, 2 mM NaPPi, 1 μg/ml pepstatin A, 2.5 μg/ml aprotinin, 5μg/ml leupeptin, 0.5 mM phenymethylsulfonyl fluoride, 0.125 mM Na_3VO_4, 25 mM NaF, and 10 μM lactacystin). The protein concentration was determined with a bicinchoninic acid (BCA) protein assay (Pierce Biotechnology, Rockford, IL, USA). Equal protein concentrations of each sample were mixed with sample buffer, loaded, and separated by sodium dodecyl sulfate-polyacrylamide gel electrophoresis (SDS-PAGE) on a 10 % (v/v) resolving gel. The proteins that were separated by SDS-PAGE were transferred to an Immobilon-P membrane (Millipore Corp., Billerica, MA) and were probed with antibodies against collagen type II, SOX-9, aggrecan, N-cadherin, AKT, phosphorylated AKT (p-AKT), peroxisome proliferator-activated receptor gamma (PPARγ), osteocalcin (OC), osteopontin (OP), p38, and phosphorylated p38 (p-p38) (all products from Abcam). β-actin (Abcam) served as the internal control.

2.9. Statistical Analysis

Quantitative data were expressed as the mean ± standard deviation. Statistical analysis was performed by ANOVA using a Bonferroni test. A *p*-value of less than 0.05 was considered to be statistically significant.

3. Result and Discussion

3.1. Enhanced *in vitro* Chondrogenic Differentiation by the Spheroid Culture of hASCs

The suspension culture of hASCs in spinner flasks induced spheroid formation (Figure. 3.2. A). Immunohistochemical analysis for caspase-3 indicated that the cells were viable in spheroids even after 14 days of culture (Figure. 3.2. B). hASC spheroids cultured in spinner flasks showed significantly less caspase-3 activity compared to hASC pellets cultured statically (Figure. 3.3.). Qualitative analysis with RT-PCR and immunohistochemistry and quantitative analysis with real-time PCR and western blotting showed that the spheroid culture of hASCs in differentiation medium with TGF-β3 resulted in enhanced chondrogenic differentiation, which was indicated by the enhanced expression of SOX-9, aggrecan and collagen type II compared with the monolayer culture (Figure. 3.4.-7.). TGF-β3 supplementation was required for the chondrogenic differentiation of hASCs *in vitro*.

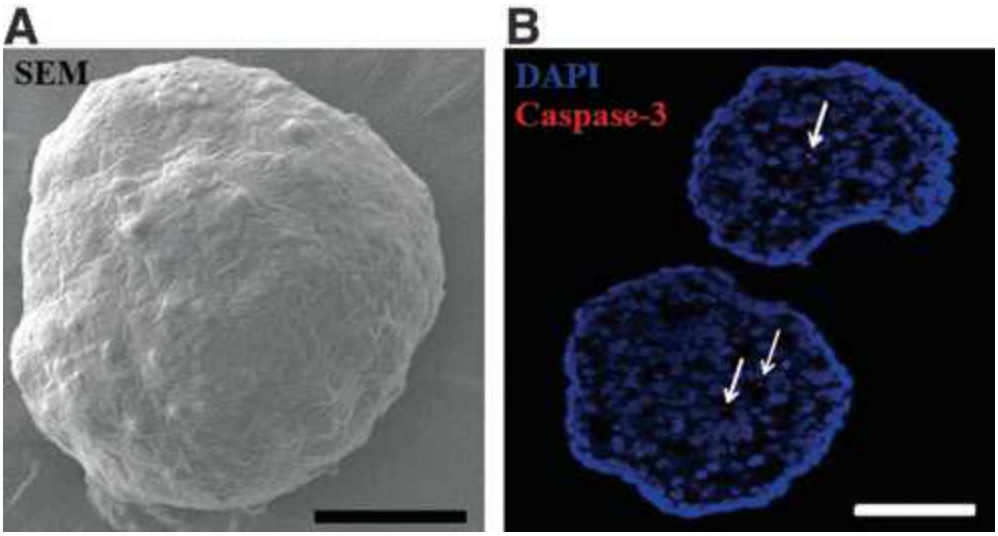

Figure. 3.2. A spheroid of hASCs at 14 days of culture. (A) an SEM image. (B) The staining for nuclei with DAPI (blue) and caspase-3 (red). The hASC spheroids had a low level of apoptotic activity. The scale bars indicate 100 μm.

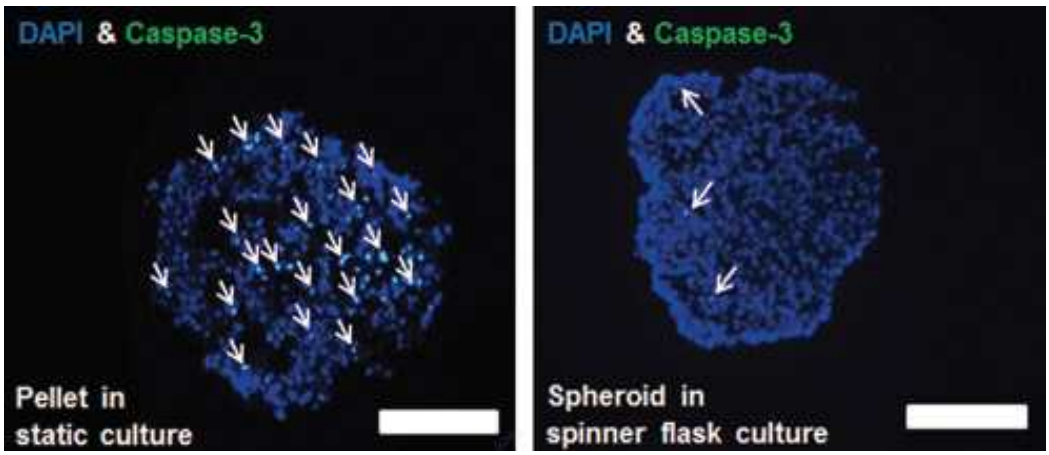

Figure. 3.3. Comparison of apoptotic activity of hASCs cultured in spheroids in spinner flasks and hASC pellets cultured statically, as evaluated by immunohistochemistry for caspase-3. The staining for nuclei with DAPI (blue) and caspase-3 (green). The arrows indicate caspase-3-positive cells. The scale bars indicate 150 μm.

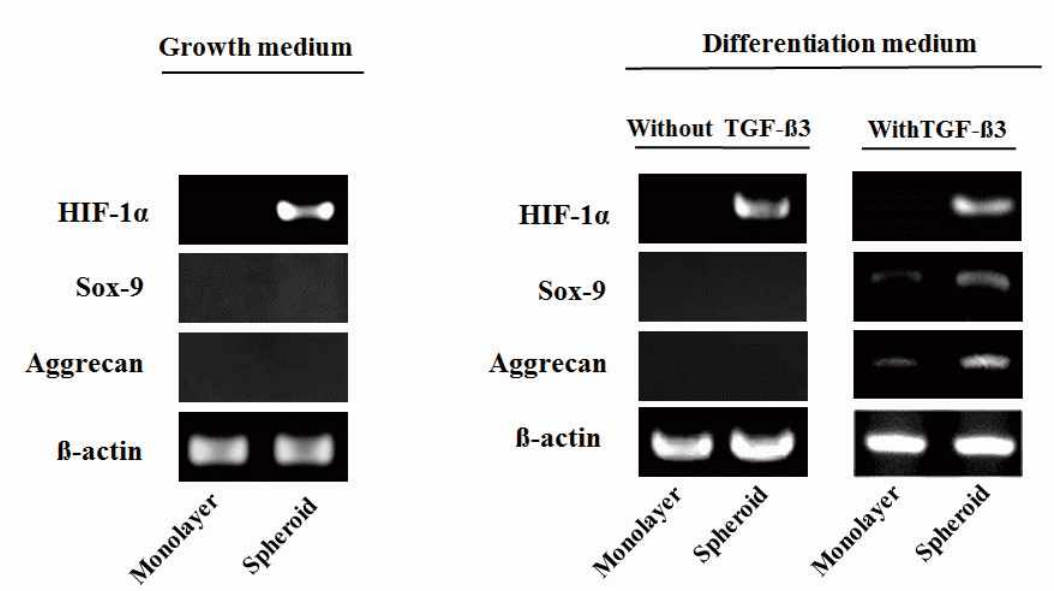

Figure. 3.4. The expression of HIF-1α and the chondrogenic differentiation-related genes in hASCs as evaluated by RT-PCR. The hASCs were cultured for 14 days in either growth medium or differentiation medium with or without TGF-β3.

3.2. The Mechanisms for Enhanced Chondrogenic Differentiation

The spheroid culture showed a dramatic increase in the expression of HIF-1 α in hASCs compared with that of the monolayer culture, regardless of the type of medium used (Figure. 3.4.). To verify the induction of chondrogenesis by hypoxia, the expression of pAKT and p-p38, which are known to be involved in chondrogenesis promoted by hypoxia,[99] was assessed through western blot analysis. Although AKT expression was observed in all of the cultures, pAKT expression was significantly higher in the spheroid culture (Figure. 3.6.). The expression of p-p38 was also significantly higher in the spheroid culture than in the monolayer culture (Figure. 3.7.). To verify the auto-induction of TGF-β3, PCR analysis was performed, and the results denoted enhanced mRNA expression of TGF-β3 in the spheroid culture with TGF-β3 supplementation (Figure. 3.8.). The expression of N-cadherin was significantly higher in the spheroid culture than it was in the monolayer culture, which indicates the presence of enhanced cell-cell interactions in the spheroid culture (Figure. 3.7.).

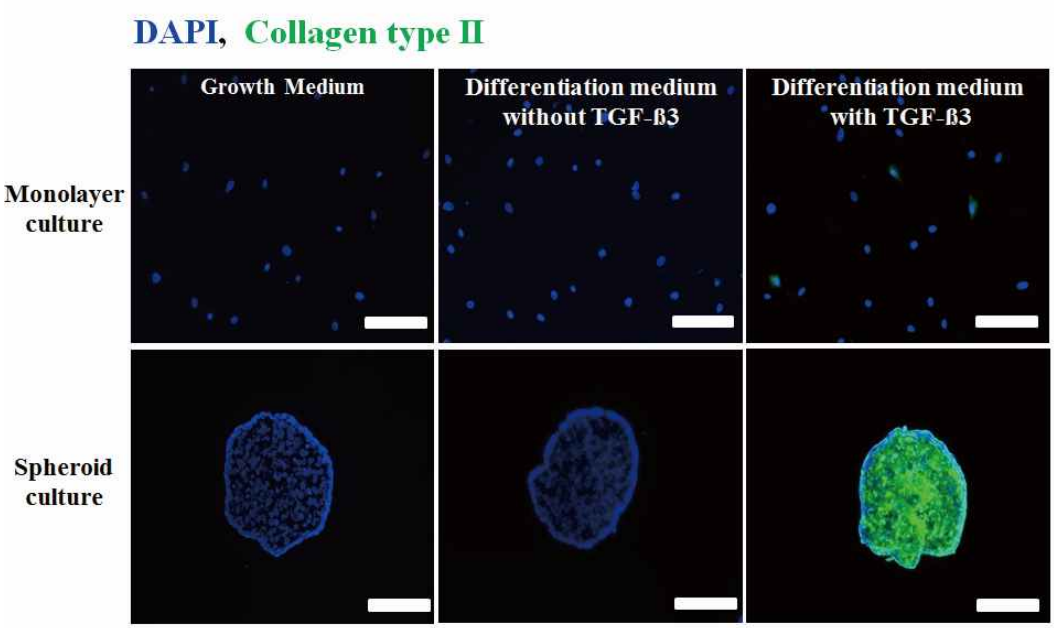

Figure. 3.5. The chondrogenic differentiation of hASCs as evaluated by immunohistochemistry for type II collagen. Type II collagen and nuclei were stained green and blue, respectively. The hASCs were cultured for 14 days in either growth medium or differentiation medium with or without TGF-β3. All of the scale bars indicate 100 μm.

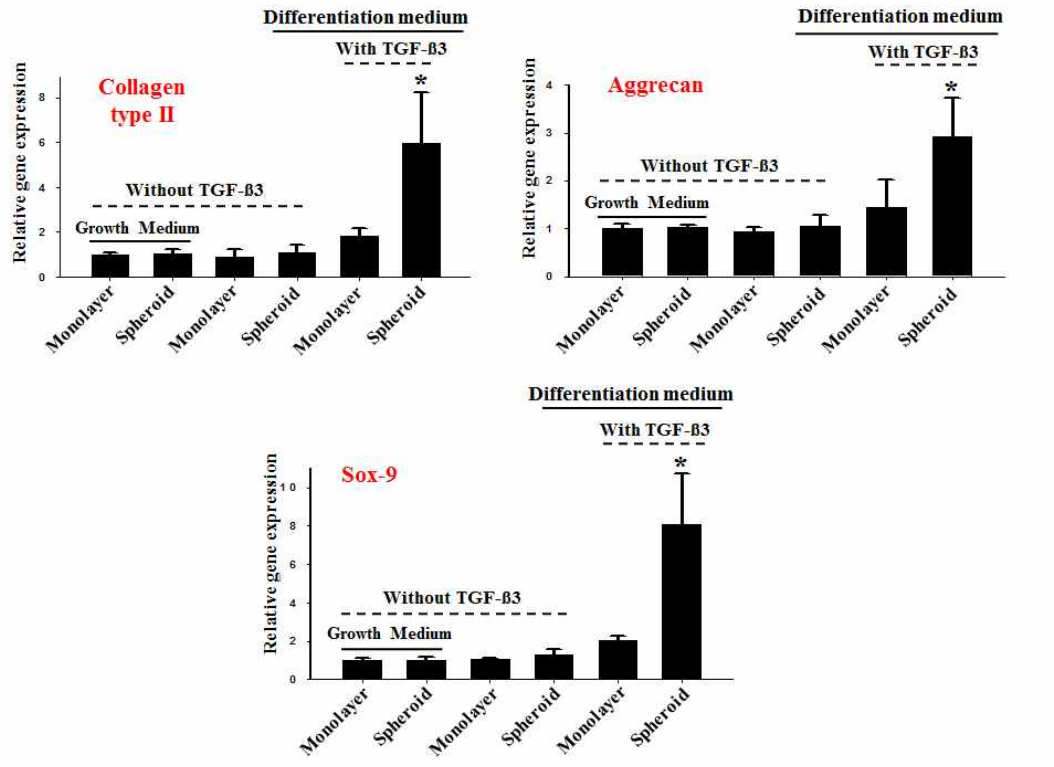

Figure 3.6. The expression of the chondrogenic differentiation-related genes in hASCs as evaluated by real-time PCR. The hASCs were cultured for 14 days in either growth medium or differentiation medium with or without TGF-β3. *p < 0.05 compared to any group.

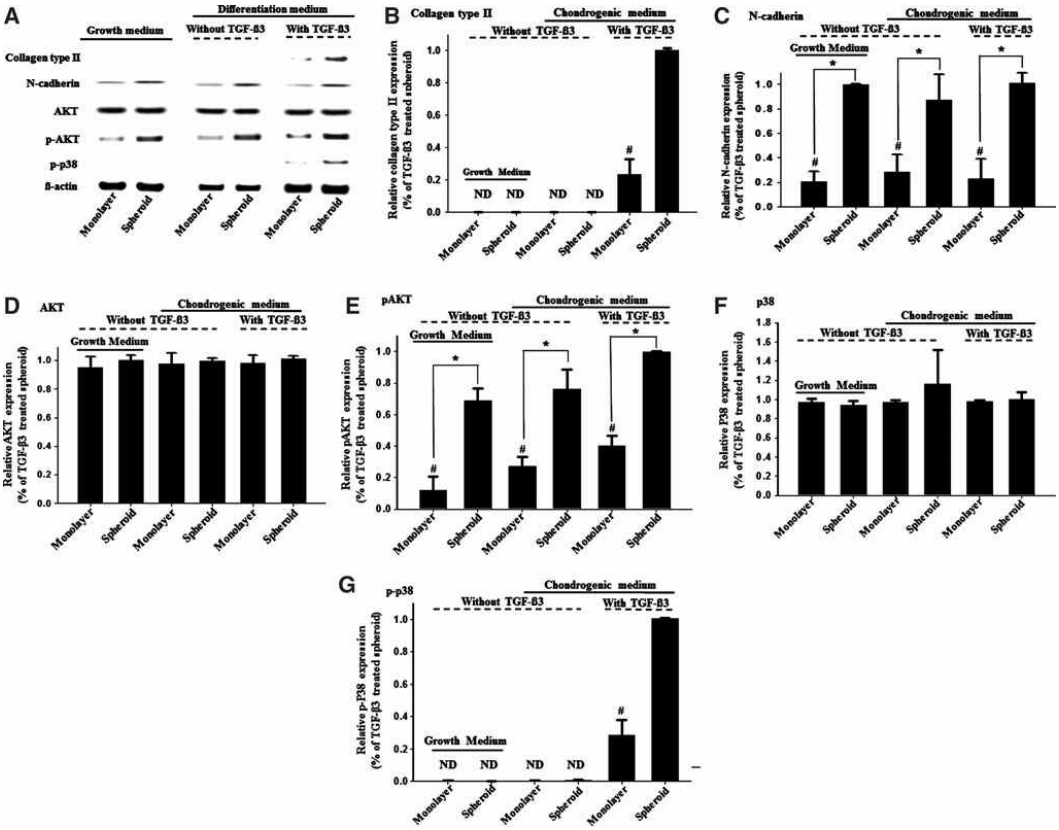

Figure. 3.7. The expression of the chondrogenic differentiation- and mechanism-related genes in hASCs as evaluated by (A) western blot analysis and (B-G) respective quantification (n = 3). The hASCs were cultured for 14 days in either growth medium or differentiation medium with or without TGF-β3. ND: not detected. *$p < 0.05$. #$p < 0.05$ compared to any group.

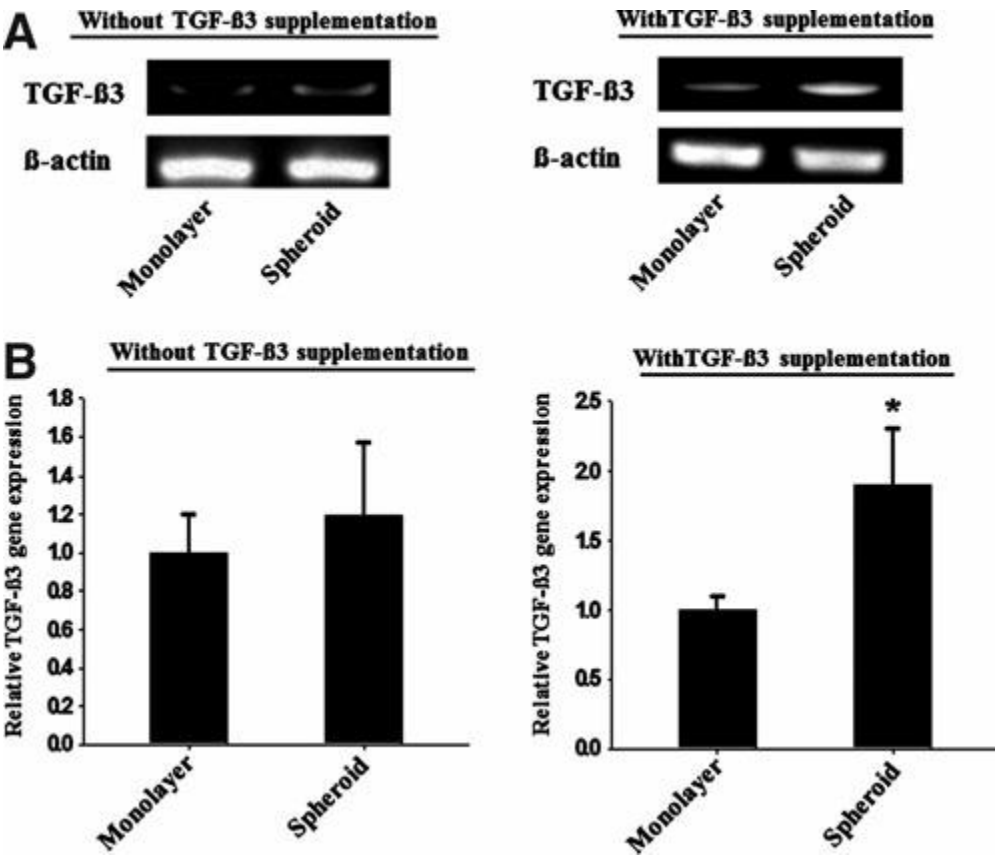

Figure. 3.8. The expression of TGF-β3 mRNA in hASCs as evaluated by (A) RT-PCR and (B) real time-PCR (n = 3). The hASCs were cultured for 14 days in either growth medium or differentiation medium with or without TGF-β3. *p < 0.01 compared to other group.

3.3. Enhanced *in vivo* Cartilage Formation by the Spheroid-cultured hASCs

The H&E and alcian blue staining indicated the lacunae structure and enhanced deposition of glycosaminoglycan in the implants of spheroid-cultured hASCs supplemented with TGF-β3 (Figure. 3.9.). Extensive alcian blue staining was observed only in the spheroids with TGF-β3. Immunohistochemical analysis indicated a greater deposition of type II collagen in the implants of spheroid-cultured hASCs supplemented with TGF-β3 than in the implants of monolayer-cultured hASCs with TGF-β3 (Figure. 3.11.). RT-PCR and western blot analyses indicated the expression of type II collagen, SOX-9 and aggrecan, at both the gene and protein levels, to be the highest in the implants of spheroid-cultured hASCs supplemented with TGF-β3 (Figure. 3.11.). To determine whether the implanted hASCs underwent adipogenesis or osteogenesis, the expression of PPARγ, OC, and OP were assessed by RT-PCR and western blot analysis. Such a differentiation tendency was not observed (Figure. 3.11.).

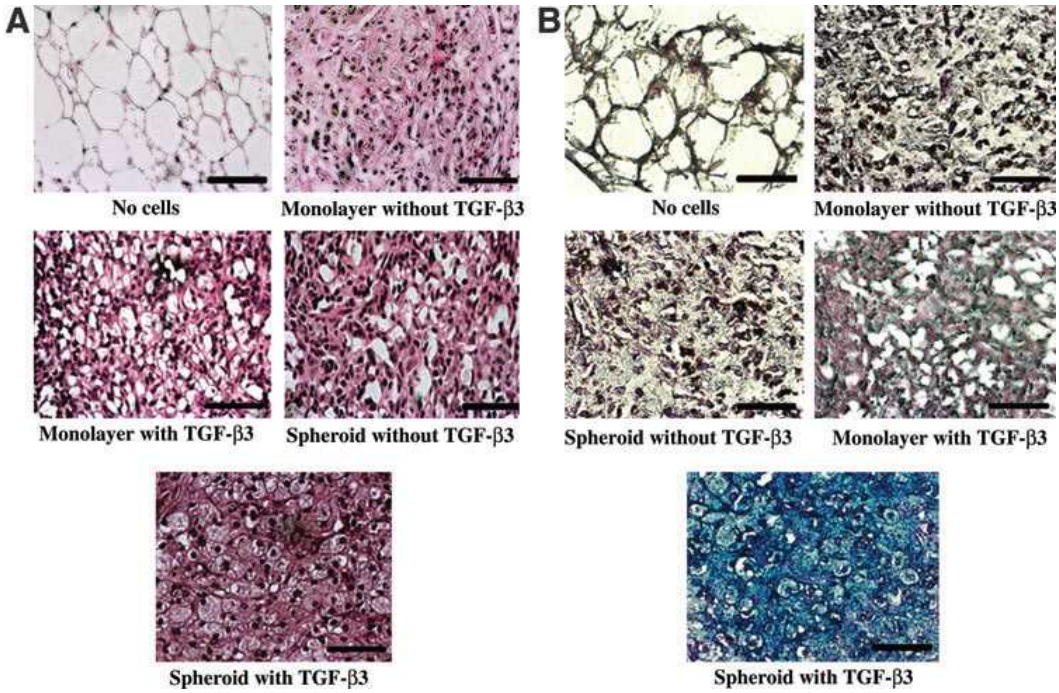

Figure. 3.9. The *in vivo* cartilaginous tissue formation by the transplantation of hASCs, cultured in a monolayer or in spheroids in differentiation medium with or without TGF-β3 and mixed with fibrin gel, into the subcutaneous space of athymic mice for 4 weeks, as evaluated by histological analysis with (A) H&E staining and (B) alcian blue staining. All of the scale bars indicate 100 μm.

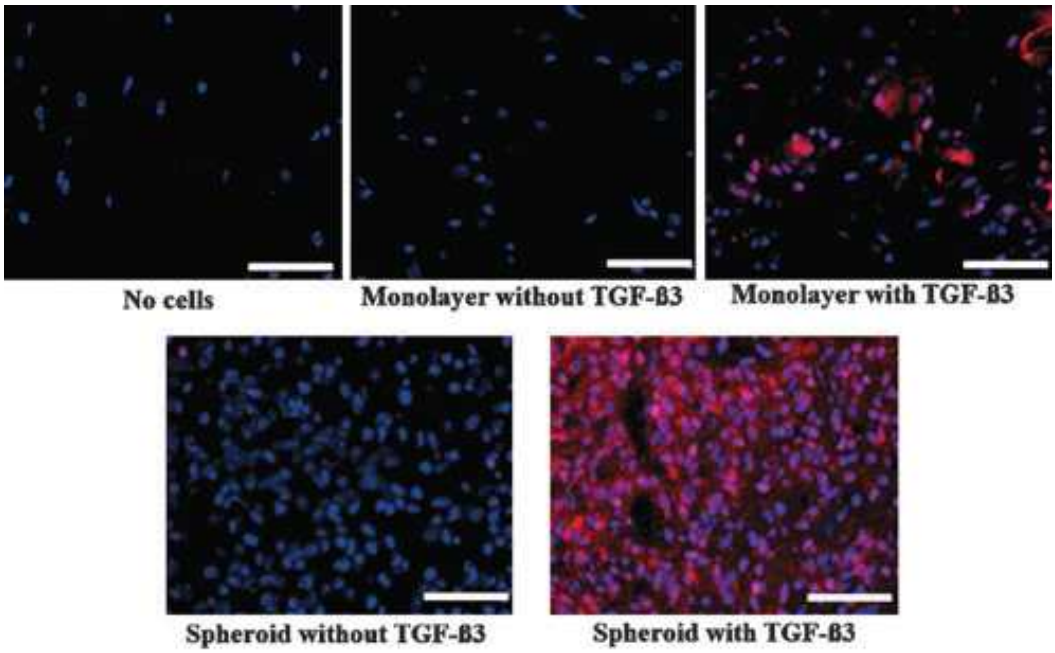

Figure. 3.10. The *in vivo* cartilaginous tissue formation by the transplantation of hASCs, cultured in monolayer or spheroids in differentiation medium with or without TGF-β3 into the subcutaneous space of athymic mice for 4 weeks, as evaluated by immunohistochemistry for type II collagen (red). The nuclei were stained with DAPI (blue). All of the scale bars indicate 100 μm.

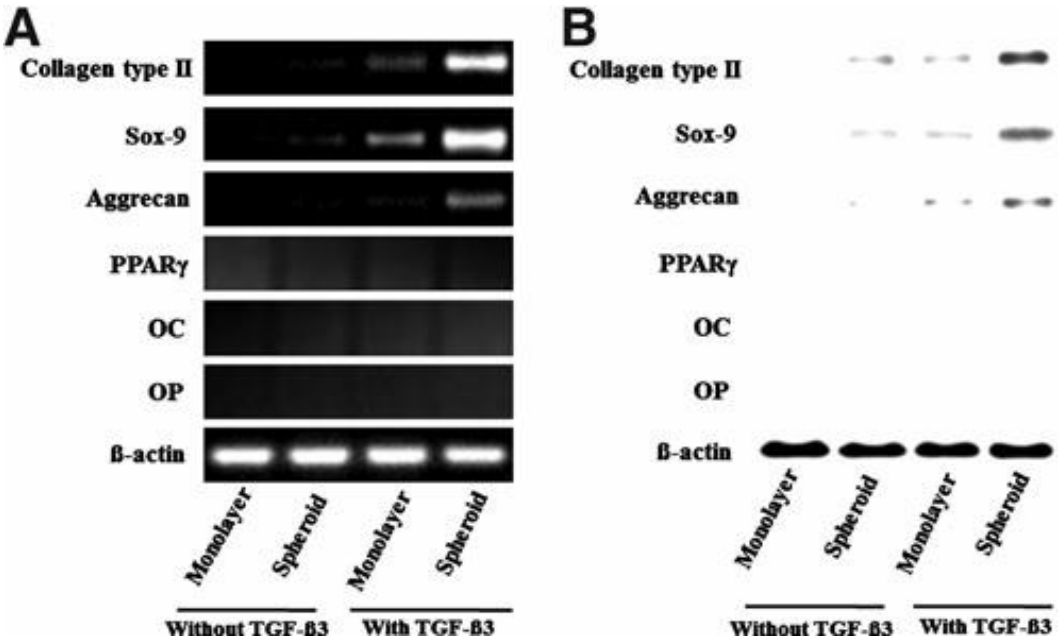

Figure. 3.11. The expression of chondrogenic, adipogenic and osteogenic differentiation markers in the tissues formed by the transplantation of hASCs, cultured in monolayer or spheroids in differentiation medium with or without TGF-β3, into the subcutaneous space of athymic mice for 4 weeks, as evaluated by (A) RT-PCR and (B) western blot analysis.

3.4. Discussion

The aim of this study was to evaluate the feasibility of the large-scale culture of hASCs for chondrogenic differentiation and to elucidate the mechanisms for enhanced chondrogenesis in hASC spheroid culture. The results demonstrated an enhanced *in vitro* chondrogenic differentiation of hASCs in a spheroid culture system and the subsequent *in vivo* cartilage formation compared with the monolayer culture. The mechanisms for the enhanced chondrogenesis involved hypoxia-induced cascades and enhanced cell-cell interactions in the spheroids (Figure. 3.12.).

One advantage of the method of spheroid culture using suspension bioreactors over the conventional monolayer culture and the pellet culture is the ease of scale-up. To produce large quantities of cells that are required for clinical applications (5.2×10^6 to 7.5×10^7 chondrocytes per defect).[100] hASCs can be cultured as spheroids for chondrogenic differentiation in a spinner flask. In contrast, only one pellet can be formed and cultured per tube in the conventional pellet culture, which is not appropriate for large-scale culture for chondrogenic differentiation. Additionally, a previous study reported extensive apoptosis of BMMSCs cultured as pellets for chondrogenic differentiation.[101] Surprisingly, spheroid culture in spinner flasks reduced apoptosis of hASCs as compared to pellet culture (Figure. 3.3.). This could be due to improved mass transfer in spinner culture compared to static pellet culture. Therefore, the spheroid culture system has the potential to decrease the labor-intensity, enhance cell viability and simplify the culture process to acquire a sufficient number of cells for clinical applications for cartilage tissue engineering.

Another advantage of the spheroid culture over the monolayer culture is the greater extent of cell-cell interactions. N-cadherin, a molecule for cell-cell

adhesion, is involved in mesenchymal chondrogenesis. It was previously shown that the inhibition of N-cadherin with neutralizing antibodies disabled the condensation of mesenchymal cells *in vitro* and *in vivo* and the subsequent chondrogenesis.[102] Through N-cadherin, the spheroid enhances the cell-to-cell interactions that are analogous to the interactions that occur in precartilage condensation development.[103] Therefore, a more condensed state can be obtained through spheroid culture system, which may be sufficient external stimulants for hASCs to undergo chondrogenesis.

The cells beneath the surface of the spheroids are generally exposed to mild hypoxia, due to the diffusion limitations of oxygen.[104] The hypoxic condition seems to present a more favorable micro environment for chondrogenesis by hASCs. This environment induces a significant expression of HIF-1α in cells in spheroids, even under normoxic culture conditions (Figure. 3.4.). HIF-1α is a component of the intrinsic ability of cells to respond to a low oxygen environment. Given that cartilage tissue resides in a low oxygen environment, HIF-1α is thought to play a key role in maintaining the chondrocyte phenotype under such a condition.[105] The activation of HIF-1α is known to stimulate the production of SOX-9, which is a chondrogenic transcription factor.[106] Although the major cartilage matrix genes such as collagen type II and aggrecan, are not directly upregulated by HIF1-α, their expression is upregulated by hypoxia through SOX-9 [92,107] A previous study has also demonstrated that the ability of hypoxia to transactivate the SOX-9 promoter was almost completely abolished by the deletion of the HIF-1α consensus sites within the SOX-9 proximal promoter.[108] Indeed, the expression of collagen type II and aggrecan were upregulated in the spheroid hASCs compared with the hASCs in monolayer culture (Figure. 3.4-7.), and the monolayer cultured hASCs, which showed no HIF-1α expression, were unable to support the enhancement of chondrogenesis.

The upregulation of phosphorylated p38, AKT, and HIF-1α that was observed in the hASC spheroid culture (Figure. 3.4. and 3.7.) suggests that the enhanced chondrogenesis in the spheroid culture of hASCs involves hypoxia and p38 and AKT signaling. Also, p38, one of the major subtypes of mitogen-activated protein kinase (MAPK), and AKT, a downstream molecule of the phosphatidylinositol 3-kinase (PI3K) pathway, are among the most widespread signaling molecules that have been identified to be implicated in chondrocyte differentiation.[108] The p38/MAPKs cascade has been established as a positive regulator in chondrogenesis by mesenchymal progenitor cells[109] and was reported to regulate TGF-β-induced chondrogenesis by human mesenchymal progenitor cells.[25] Inhibition of the p38/MAPKs cascade with pharmacological inhibitors suppressed cartilage matrix production.[108] It was previously reported that p38 and AKT are upregulated during hypoxic conditions, and this condition upregulates chondrogenesis in rat mesenchymal stem cells.[99] In this study we showed that HIF-1α was expressed only in the spheroid-cultured hASCs (Figure. 3.4.) and that pAKT was upregulated in the spheroid-cultured hASCs compared with monolayer-cultured hASCs. Also, p-p38 expression was significantly higher in the spheroid-cultured hASCs compared with that observed in the monolayer-cultured hASCs (Figure. 3.7.).

The expression of TGF-β3, a chondrogenic factor, was enhanced in hASCs that were cultured as spheroids, which is the cause of the enhanced chondrogenesis by hASCs cultured as spheroids (Figure. 3.8.). The mechanisms for the enhanced expression of TGF-β3 involved p38 and the autocrine action of TGF-β3 (Figure. 3.12.). It was reported that the upregulation of HIF-1α activates p38 by facilitating its phosphorylation.[99] The activated p38, in turn, activates TGF-β3 expression.[111] Also, expressed TGF-β3 acts as an autocrine factor to induce p38 activation.[111] Our data (Figure. 3.4., 3.7., and 3.8.) suggest that the hypoxic environment in spheroids enhances TGF-β3 expression through

p38 activation, to induce enhanced chondrogenesis by hASCs cultured in spheroids.

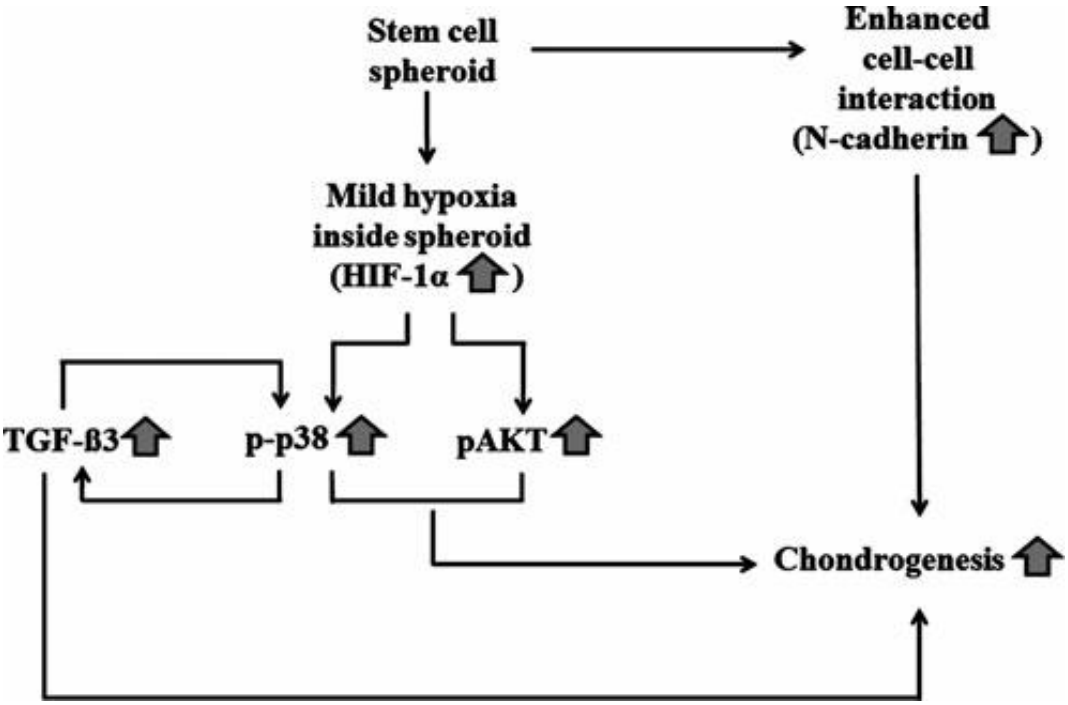

Figure. 3.12. A schematic diagram of the mechanisms for the enhanced chondrogenic differentiation of hASCs through spheroid cultivation

4. Conclusion

The culture of hASCs as spheroids in large-scale suspension bioreactors (i.e. spinner flasks) promoted chondrogenic differentiation. Unlike pellet culture, culture using spinner flasks is easily scalable and may be useful for the clinical application of hASCs in cartilage regeneration, which requires a large-scale culture of cells. The mechanisms for the enhanced chondrogenesis in the hASC spheroid cultures involve hypoxia-related cascades and enhanced cell-cell interaction.

Chapter 4

Dual roles of graphene oxide in chondrogenic differentiation of adult stem cells: cell-adhesion substrate and growth factor-delivery carrier

1. Introduction

Graphene (G) and its derivatives are being explored for use in various biomedical applications such as drug delivery,[112] imaging,[113] and photo thermal cancer therapy.[114,115] Furthermore, studies are expanding in the field of regenerative medicine, because these materials are capable of influencing cellular behaviors such as the adhesion,[116] growth,[116] and differentiation of stem cells.[116-119] It was reported that G induced the osteogenesis of human mesenchymal stem cells (hMSCs)[116] and the differentiation of human neural stem cells into neurons,[117] while graphene oxide (GO) induced differentiation of hMSCs to adipocytes[116] and myoblasts.[118] The previous studies indicate that G and GO have distinct properties when utilized as substrates for stem cell culture and differentiation. For example, GO showed higher protein adsorption compared with G.[116] Although they both enhanced cell adhesion and growth, proteins such as insulin interacted with G and GO in different manners.[116] GO formed an electrostatic interaction with insulin and preserved the protein structure, while G denatured the native structure. Because the insulin protein structure was preserved on GO, the adipogenic differentiation of hMSCs was significantly enhanced when cultured on GO compared with G.[116] Although many studies have explored how various properties of G and GO differentiate adult stem cells,[116-119] there has been no report on the use of G or GO for chondrogenic differentiation. This study reports, for the first time, the use of GO for the chondrogenic differentiation of stem cells.

The chondrogenic differentiation of adult stem cells is conventionally achieved through the culture of cells in pellets.[120] Cell condensation into pellets mimics the chondrogenic progenitor cell derivation during embryogenesis through cell condensation.[121] However, because the major composition of the pellets is

cells and the extracellular matrix (ECM) amount is negligible, the cell-ECM interaction that promotes chondrogenic differentiation[122] is absent. Additionally, the diffusional limit of approximately 150–200 μm restricts the mass transportation of many molecules, including oxygen, into the pellets.[123] Such characteristics thus limit the size of the pellets because pellets larger than the diffusional limit display a necrotic core surrounded by a viable cell layer. To overcome such hurdles, we used GO sheets as both a cell-adhesion substrate and a chondrogenic inducer-delivery carrier for *in vitro* chondrogenic differentiation of human adipose-derived stem cells (hASCs) in pellets in this study (Figure. 4.1.). GO sheets (size = 0.5-1 μm) were utilized to adsorb fibronectin (FN, a cell-adhesion protein) and transforming growth factor-β3 (TGF-β3) (a chondrogenic inducer) and were then incorporated into hASC pellets. The adsorption of FN and TGF-β3 on GO sheets relies on the surface chemistry of GO. GO features both hydrophobic π domains and carboxylic and hydroxyl groups. The π-electron clouds in the GO sheets are capable of interacting with the inner hydrophobic cores of FN and TGF-β3 proteins. These proteins can also be adsorbed through electrostatic interaction with the carboxylic and hydroxyl groups of GO. It was reported previously that hydroxyl groups strongly adsorb FN compared with other chemical groups.[124] Dispersion of FN- and TGF-β3-adsorbed GO sheets in hASC pellets may enhance chondrogenic differentiation of hASCs by adding a cell-FN interaction and supplying TGF-β3 effectively (Figure. 4.1.).

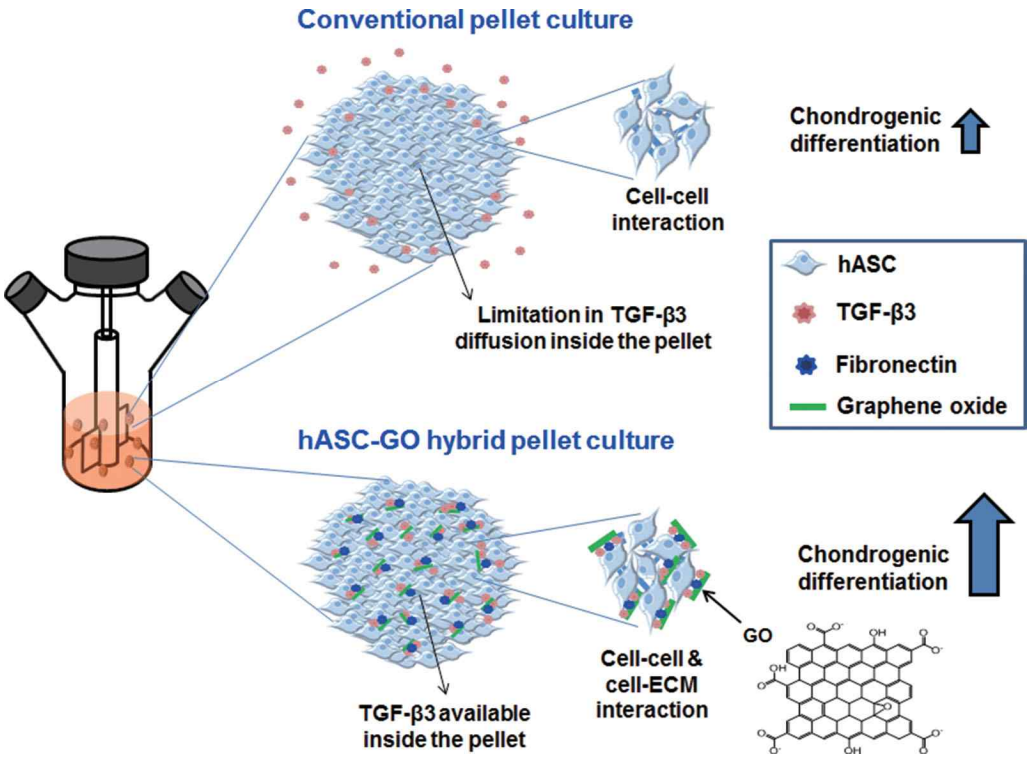

Figure. 4.1. A schematic diagram describing the enhancement in chondrogenic differentiation of hASCs using GO. The conventional pellet culture provides only cell-cell interaction, and TGF-β3 diffusion inside the pellets is often limited; both of these factors limit the chondrogenic differentiation of stem cells. To improve chondrogenic differentiation, stem cells can be cultured in hybrid pellets of hASCs and GO. GO sheets are adsorbed with cell-adhesion proteins (e.g. FN) and TGF-β3 and dispersed in hASC pellets, providing cell-ECM interactions and TGF-β3 to enhance the chondrogenic differentiation of hASCs.

2. Materials and Method

2.1 GO Synthesis and Characterization

GO sheets were prepared as described previously using the modified Hummers method.[144] After synthesis, GO sheets were carefully separated by the centrifugation of the GO solution at 4000 rpm for 30 min three times, and then, the transparent brown upper solution of GO was collected.[147] TEM analysis was conducted with a JEOL JEM-2100F transmission electron microscope operating at 200 kV. Samples were prepared by putting a drop of the particle dispersions onto a carbon-coated copper grid. The surface morphology of the GO sheets was examined with field-emission scanning electron microscopy (FE-SEM) (JEOL JSM-6700F, SE resolution: 1.0 nm (15 kV), 2.2 nm (1 kV); Accelerating voltage: 0.5 kV ~ 30 kV). The sample topography and thickness measurements of the GO sheets were performed with a Nanoscope IIIA (Digital Instruments) atomic force microscope (AFM) in tapping mode. The Raman spectra of the samples were obtained with a Raman spectrometer (T64000) at room temperature, with an excitation laser source of 514 nm. EDS (INCA Energy, Oxford Instruments Analytical LTD., Bucks, UK) was used to identify and observe the protein absorption on the GO sheets following incubation of the GO sheets in 10 % (v/v) serum-containing medium for 4 hours.

2.2 hASC Culture

hASCs were purchased from Lonza (Allendale, NJ, USA). hASCs were cultured in a growth medium consisting of α-minimum essential medium (α

-MEM, Gibco BRL, Gaithersburg, MD, USA), 10 % (v/v) fetal bovine serum (FBS, Gibco BRL), 100 units/ml of penicillin, and 100 μg/ml of streptomycin. hASCs at the fourth passage of cultivation were utilized for the experiments in this study.

2.3 hASC Pellet Formation and Chondrogenic Differentiation

To evaluate GO incorporation into hASC pellets, GO sheets were pre-labeled with DiI (6.25 mM, Invitrogen) at 4 °C for 6 hours and incorporated into pellets at 1 μg/ml concentration for 24 hours. Briefly, GO was added to DiI solution and reacted for 6 hours at 4 °C. The solution was centrifuged at 13000 rpm and the supernatant containing unabsorbed DiI was discarded. The collected GO was gently washed twice with distilled water prior to use for pellet incorporation. To adsorb TGF-β3 first and FN second on GO sheets, GO sheets were suspended in distilled water containing TGF-β3 (600 ng) at a concentration of 1 μg/ml and incubated at 4 °C for 4 hours. Following the incubation, an ELISA preformed with the supernatant indicated that all TGF-β3 was adsorbed on the GO sheets. TGF-β3-adsorbed GO sheets were then incubated in α-MEM containing 10 % (v/v) FBS for 4 hours to allow FN from the serum to be adsorbed on the GO sheets. GO sheets reacted only with α -MEM was used as another group. The hanging-drop method was used to form pellets as previously described[148] with a cell concentration of 3x106 cells / ml and a GO concentration of 1μg / ml in the cell suspension. Conventional pellet culture without GO sheets was used as a control. After 24 hours of pellet formation, cell viability and apoptosis were evaluated using FDA-EB (Sigma) and a TUNEL assay kit (Millipore Corp., Billerica, MA). For the FDA-EB assay, pellets were incubated with a FDA-EB (5 μg/ml and 10 μg /ml,

respectively) solution for 5 minutes at 37 ℃ and then washed three times with phosphate-buffered saline (PBS). Dead cells were stained red due to the nuclear permeability of EB. The viable cells, which are capable of converting the non-fluorescent FDA into fluorescein, were stained green. Formed pellets were transferred to spinner flasks (working volume = 100 ml, Wheaton, Millville, NJ, USA), which were siliconized with sigmacoat (Sigma, St. Louis, MO, USA) to prevent cell adhesion onto the flask walls before use. A chondrogenic medium consisting of Dulbecco's modified Eagle's medium high glucose (Gibco BRL), 50 mg/ml of ascorbic acid, and 100 nM of dexamethasone supplemented with 10 ng/ml of TGF-β3 (R&D systems, Minneapolis, MN, USA) was used, and cells were cultured at 40 rpm. For pellets containing TGF-β3-adsorbed GO sheets, TGF-β3 was not added to the chondrogenic medium. Medium was changed every other day for 14 days.

2.4 TEM Analysis

The pellets and hybrid pellets were fixed with Karnovsky's solution (EMS, Hatfield, PA, USA) for 24 hours at 4 °C and washed 3 times with a 0.05 M sodium cacodylate buffer. Then, the specimens were fixed with 2 % osmium tetraoxide (Sigma) for 2 hours at 4 °C, washed three times with cold distilled water, dehydrated through a series of graded ethanol (50, 60, 70, 80, 90, 95, 98, and 100 %) and propylene oxide rinses, and finally embedded in Spurr's resin. The samples were then polymerized at 60 °C for 24 hours and cut into thin slices using an ultramicrotome (MTX, RMC, Arizona, USA). The thin sections were observed with a Libra 120 microscope (Carl Zeiss, Oberkochen, Germany).

2.5 SEM Analysis

The pellets and hybrid pellets were washed twice with PBS, prefixed with 4 % (v/v) buffered glutaraldehyde (Sigma) for 1 hour, and fixed with 0.1 % (v/v) buffered formaldehyde (Sigma) for 24 hours. The fixed specimens were dehydrated in ascending grades of ethanol, dried, and mounted on aluminum stubs. The specimens were subsequently coated with platinum using a Sputter Coater (Cressington 108, Cressington Scientific Instruments, Cranberry, PA, USA) and examined with SEM (JSM-6330F, JEOL).

2.6 Histology and Immunocytochemistry

Pellets were harvested on day 14. The specimens were fixed in 10 % (v/v) buffered formaldehyde, dehydrated in a graded ethanol series, and embedded in paraffin. The specimens were sliced into 4-μm sections. The sections were stained with safranin-O and alcian blue for glycosaminoglycan detection. The sections were also stained with anti-type II collagen and anti-TGF-β3 antibodies and counter-stained with 4,6 diamidino-2-phenylindole (DAPI, Vector Laboratories, Burlingame, CA, USA) for immunocytochemical analysis. Unless otherwise mentioned, all antibodies were purchased from Abcam (Abcam, Cambridge, UK). Aggrecan was detected using a human aggrecan antibody (Abcam). Staining was visualized with an avidin-biotin complex immunoperoxidase (Vetastain® ABC kit, Vector Laboratories) and a 3,3'-diaminobenzidine substrate solution kit (Vector Laboratories). Cell nuclei were counter stained with hematoxylin. All images were taken with a fluorescence microscope (Olympus IX71, Olympus, Tokyo, Japan).

2.7 RT-PCR Analysis

Samples were lysed with TRIzol reagent (Invitrogen, Carlsbad, CA, USA). The total RNA was extracted with chloroform (Sigma) and precipitated with 80 % (v/v) isopropanol (Sigma). After the supernatant was removed, the RNA pellet was washed with 75 % (v/v) ethanol, air-dried, and dissolved in 0.1 % (v/v) diethyl pyrocarbonate-treated water (Sigma). The RNA concentration was determined by measuring the absorbance at 260 nm with a spectrophotometer. Reverse transcription was performed with 5 μg of pure total RNA and SuperScriptTM II reverse transcriptase (Invitrogen) and was followed by PCR amplification of the synthesized cDNA. The PCR consisted of 35 cycles of denaturing (94 °C, 30 sec), annealing (58 °C, 45 sec), and extension (72 °C, 45 sec), with a final extension at 72 °C for 10 min. The PCR was followed by electrophoresis on a 2 % (w/v) agarose gel and DNA visualization by ethidium bromide staining. The PCR products were analyzed with a gel-documentation system (Gel Doc 1000, Bio-Rad, Hercules, CA, USA).

2.8 Real time-PCR Analysis

Total RNA was extracted at day 14 using 1 ml of TRIzol reagent (Invitrogen) and 200 μl of chloroform. The samples were centrifuged at 12,000 rpm for 10 min at 4 °C. The RNA pellets were washed with 75 % (v/v) ethanol and dried. After the drying procedure, the samples were dissolved in RNase-free water. The iQ™ SYBR Green Supermix kit (Bio-Rad Laboratories, Hercules, CA, USA) and the MyiQ™ single color Real-Time PCR Detection System (Bio-Rad Laboratories) were used.

Table 1. Primer sequences for RT- and real-time PCR

p53	Sense	5′-CGG GAT CCA TGG AGG AGC CGC AGT CAG AT-3′
	Antisense	5′-CCG CTC GAG TTT CTG GGA AGG GAC AGA AGA-3′
SOX-9	Sense	5′-GTA CCC GCA CTT GCA CAA C-3′
	Antisense	5′-TCG CTC TCG TTC AGA AGT CTC-3′
RUNX2	Sense	5′-GCA GCA CGC TAT TAA ATC CAA-3′
	Antisense	5′-ACA GAT TCA TCC ATT CTG CCA-3′
COLLAGEN X	Sense	5′-CCC TTT TTG CTG CTA GTA TCC-3′
	Antisense	5′-CTG TTG TCC AGG TTT TCC TGG CAC-3′
AGGRECAN	Sense	5′-ACC CTG GAA GTC GTG GTG AAA-3′
	Antisense	5′-CGT GGC AAT GAT GGC ACT G-3′

2.9 ELISA for TGF-β3

The profiles of the *in vitro* release of TGF-β3 from GO sheets were determined by ELISA (R&D Systems). TGF-β3-adsorbed GO sheets were placed in culture well inserts (Transwell®, Corning, NY, USA) and immersed in PBS at 37 °C. At various time points, the supernatant was collected, and the TGF-β 3 concentration in the supernatant was determined using the ELISA kit (n = 3 per group). Briefly, the capture antibody was diluted to the working concentration in PBS without the carrier protein, immediately placed on a 96-well microplate (Corning) and incubated overnight at room temperature. The supernatant was then aspirated, and each well was washed with wash buffer and blocked by adding reagent diluents (1 % (w/v) of bovine serum albumin in PBS) to each well. After washing and adding the sample or standards to the plate, the detection antibody was added. Then, streptavidin-horseradish peroxidase was added to each well. Finally, the substrate solution was added to each well, and the 450 nm absorbance was read with a microplate reader (Powerwave, Bio-Tek, Winooski, VT, USA).

2.10 Circular Dichroism

The structure of TGF-β3 adsorbed on the GO sheets after incubation in PBS for 3 days was examined using CD (Jasco J-810, Applied Photophysics, Surrey, BA, UK) and compared with the structure of native TGF-β3 and TGF-β3 suspended in medium for 3 days. Total TGF-β3 was physically detached from the GO sheets followed by five freeze-thaw cycles at -70 °C and 37 °C. The total amount of TGF-β3 protein was quantified using the Bradford reagent (Sigma). Each CD spectrum and its corresponding high-tension voltage curve

were recorded on a Jasco J-810 spectropolarimeter using a quartz cell with an optical path length of 1 mm. The scanning speed was set at 50 nm per minute, and the wavelength range was set at 160 nm – 280 nm.

2.11 Western Blot Analysis

Samples (n = 3 per group) were lysed in ice-cold lysis buffer (15 mM Tris HCl (pH 8.0), 0.25 M sucrose, 15 mM NaCl, 1.5 mM MgCl2, 2.5mM EDTA, 1mM EGTA, 1mM dithiothreitol, 2mM NaPPi, 1μg/ml pepstatin A, 2.5 μg/ml aprotinin, 5 μg/ml leupeptin, 0.5 mM phenylmethyl sulfonyl fluoride, 0.125 mM Na3VO4,25mM NaF, and 10μM lactacystin). The protein concentration was determined with a bicinchoninic acid (BCA) protein assay (Pierce Biotechnology, Rockford, IL, USA). Equal protein concentrations of each sample were mixed with sample buffer, loaded, and separated by sodium dodecyl sulfate-polyacrylamide gel electrophoresis (SDS-PAGE) on a 10 % (v/v) resolving gel. The proteins that were separated by SDS-PAGE were transferred to an Immobilon-P membrane (Millipore Corp.) and were probed with antibodies (Abcam) against collagen type II, ERK, phosphorylated ERK (pERK), p38, phosphorylated p38 (pp38), JNK, and phosphorylated JNK (pJNK). β-actin served as the internal control. To detect FN adsorbed on GO, GO-coated titanium substrate was immersed in the serum-containing medium for 1 hour and washed 3 times with PBS. Then, the GO-coated titanium substrate was put in an ice-cold lysis buffer, and the absorbed proteins were scrapped from the GO. The buffer solution containing FN was transparent, indicating GO-free status of the sample. The sample was processed as described above for western blot analysis for FN.

2.12 Statistical Analysis

All quantitative data are expressed as the mean ± standard deviation. Statistical analysis was performed using ANOVA with a Bonferroni test. A *p*-value less than 0.05 was considered to be statistically significant.

3. Result and Discussion

3.1. Characterization of GO Sheets

Figure. 4,2. A-C displays scanning electron microscopy (SEM), transmission electron microscopy (TEM), and atomic force microscopy (AFM) images of the as-synthesized GO sheets. The GO sheets had dimensions of approximately 0.5 - 1μm (Figure. 4.2. C). Some of the GO sheets appeared to be self-folded (Figure. 4.2. A), indicating that the sheets were flexible. The TEM image and the corresponding electron diffraction pattern taken by directing the electron beam perpendicular to the flat faces of a GO sheet exhibited diffraction spots with a six-fold rotational symmetry, showing the graphene-like crystallinity of the GO (Figure. 4.2. B).[125] The AFM image analysis revealed that the GO sheets had a thickness of approximately 1.2 nm (Figure. 4.2. C). Additionally, to obtain a better understanding of the structure of the GO sheets, we conducted the Raman analysis. The characteristic peaks of the G band and D band taken from the as-synthesized GO sheets were 1590 cm^{-1} and 1350cm^{-1} (I_D/I_G ratio of 1.07), respectively, which were similar to the literature values for GO (Figure. 4.1. D).[126,127]

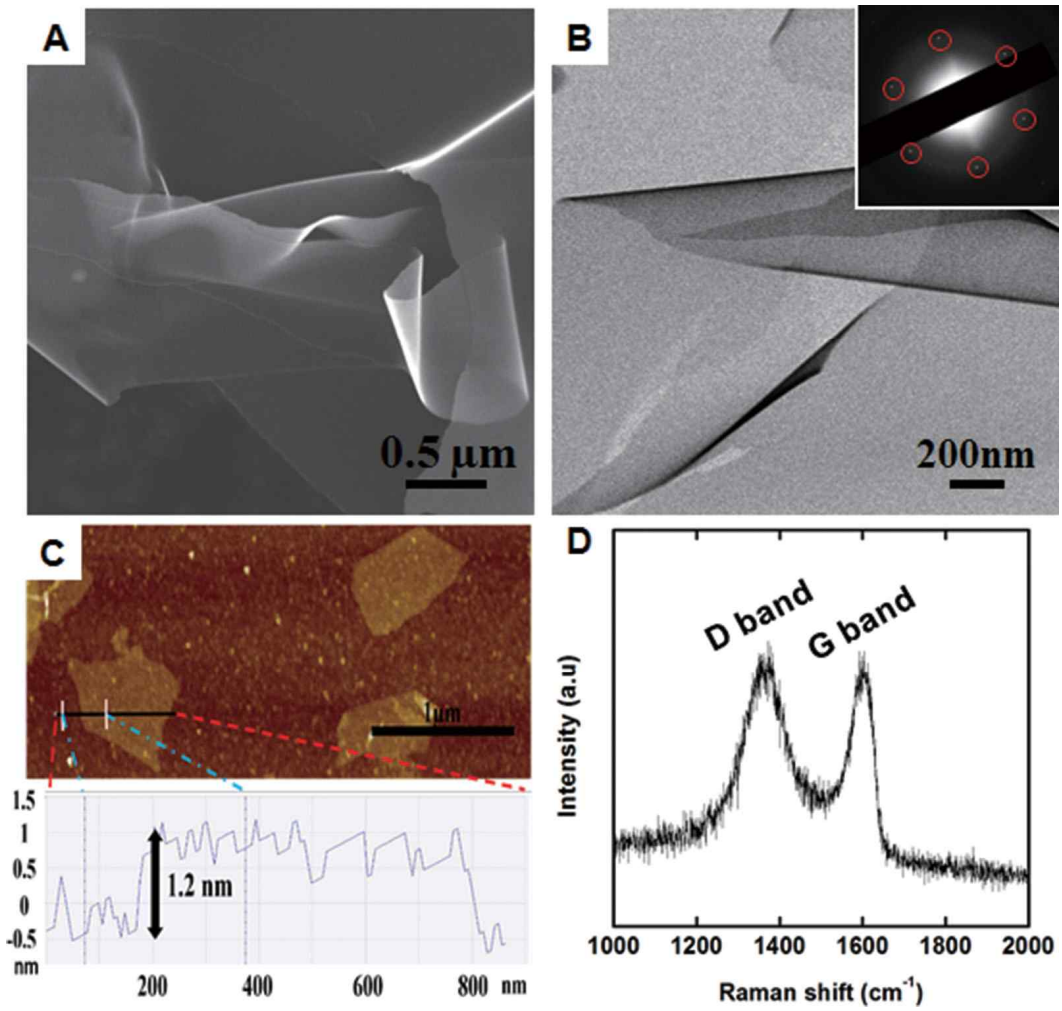

Figure. 4.2. GO characterization. (A) SEMimage.(B)TEM image and (inset) the corresponding ED pattern. (C) Tapping-mode AFM image and the height along the line shown in the AFM image. (D) Raman spectrum using 514-nm laser excitation.

3.2. GO Incorporation into hASC Pellets

To show GO incorporation into hASC pellets, SEM, TEM, and fluorescence microscopy images were acquired at day 1. In the SEM images, GO sheets were detected on the surface of the formed hybrid pellets (Figure. 4.3. A). To verify the GO distribution within the pellet, GO sheets were labeled with a fluorescent cationic dye, DiI, prior to incorporating them into the pellets. The acquired fluorescence images showed GO sheet dispersion throughout the formed pellets (Figure. 4.3. B). GO flakes at a concentration of 1 μg/ml may be hardly detectable. However, as the cells formed a pellet, the GO flakes (at 1 μg GO/ml cell-suspension volume) in the cell suspension were incorporated into the pellet and concentrated within the pellet by approximately 6 folds (GO concentration = 6 μg GO/ml pellet volume) as the pellet volume was approximately 6 folds less than the volume of cell suspension. Therefore, GO flakes in pellets (Figure. 4.3. B) were detectable as the concentration of GO flakes in the pellet would be much higher than 1 μg/ml. GO sheets are capable of quenching fluorescent dyes bound to GO sheet surface only at low concentrations of fluorescent dyes. It was reported that, at a GO concentration of 17 μg/ml, dye fluorescence was observed only at dye concentrations higher than 1.5 μM. The non-quenching effect is due to the excessive dye accumulation on GO surfaces via electrostatic and/or π- π interaction. At dye concentrations lower than 1.5 μM, dye fluorescence quenching was observed.[128] Since the fluorescent dye concentration (6.25 mM) in this study was much higher than the reported threshold dye concentration (1.5 μM) and the GO sheet concentration (1 μg/ml) used was much lower, quenching could have been negligible and thus fluorescence was observed (Figure. 4,3. B). TEM images revealed GO sheet interaction with hASCs in the hybrid pellets (Figure. 4.3. C).

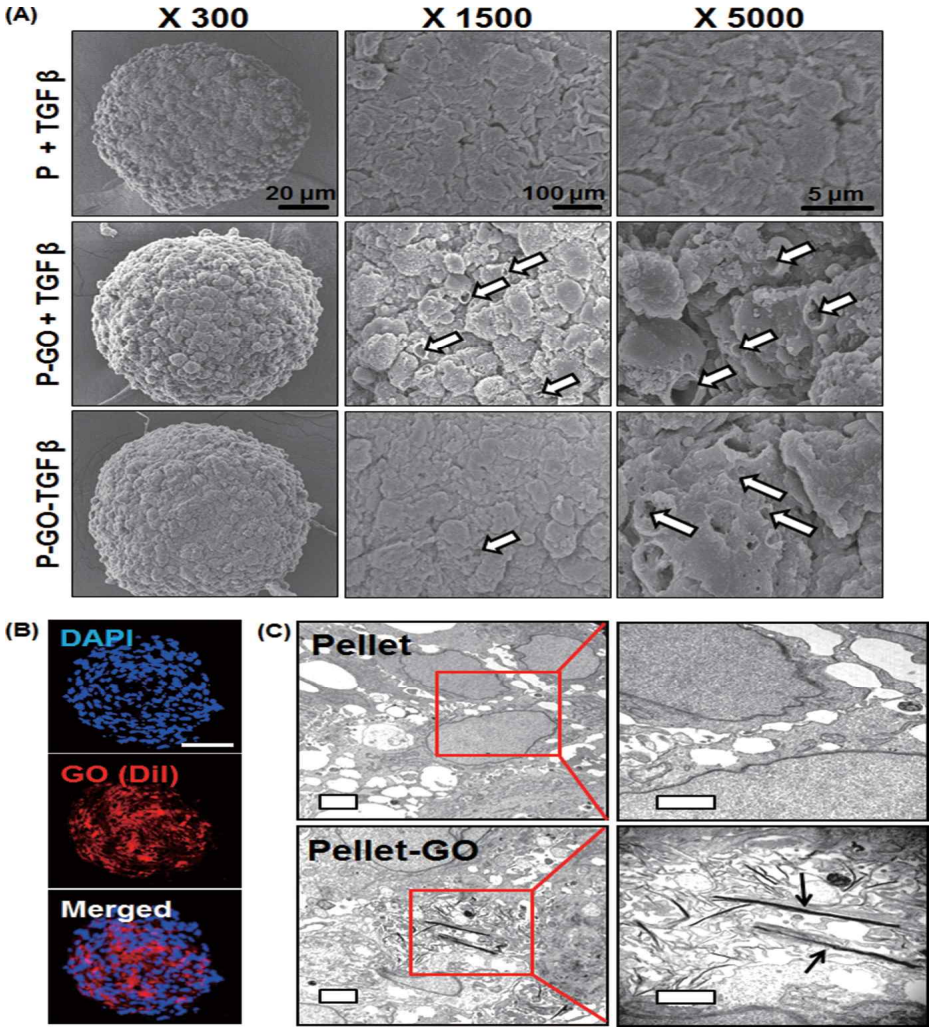

Figure. 4.3. GO incorporation into hASC pellets. (A) SEM images showing GO on the hybrid pellet surface (white arrows). P+TGF-β, hASC pellets with TGF-β3 added to the medium; P-GO+TGF-β, hybrid pellets of GO-hASCs with TGF-β3 added to the medium; P-GO-TGF-β, hybrid pellets of GO-hASCs with TGF-β3-adsorbed GO sheets. (B) Distribution of DiI-labeled GO sheets (red) in the hybrid pellet. Scale bar indicates 100μm. (C) TEM images showing GO sheets (arrows) interacting with cells in the hybrid pellet. Scale bar indicates 0.5 μm.

3.3. Cytotoxicity of GO Sheets in hASC-GO Hybrid Pellets

To determine whether GO shows cytotoxicity, the viability and apoptotic activity of hASCs after GO sheet incorporation into the hybrid pellets were examined. Cell viability was assessed using fluorescein diacetate-ethidium bromide (FDA-EB) staining. FDA-EB staining indicated no cell death for either hASC pellets or hASC-GO hybrid pellets (Figure. 4.4. A). The apoptotic activity of hASCs was assessed with a terminal deoxynucleotidyl transferase dUTP nick end labeling (TUNEL) assay and by evaluating apoptotic gene and protein expression. Apoptotic cells were rarely detected with the TUNEL assay in any of the three groups of hASC pellets: pellets with TGF-β3 added to the medium (P+TGF-β), hybrid pellets of GO-hASCs with TGF-β3 added to the medium (P-GO+TGF-β), and hybrid pellets of GO-hASCs with TGF-β3-adsorbed GO sheets (P-GO-TGF-β) (Figure. 4.4. B). Reverse transcriptase polymerase chain reaction (RT-PCR) analysis revealed that the expression of apoptotic markers, caspase-3 protein and the p53 gene did not show significant differences between groups (Figures. 4.4. C and D). These data clearly indicate no cytotoxicity of GO sheets prepared in this study. Cytotoxicity of GO has been reported previously.[129] In the previous study, GO sheets exhibit toxicity to hMSCs only at concentrations higher than 10μg/ml and at a size range of 3.8 ± 0.4 μm. However, we used GO sheets at a concentration of 1 μg/ml with a size range of 0.5 to 1 μm in this experiment, and under these conditions, GO was non-toxic.

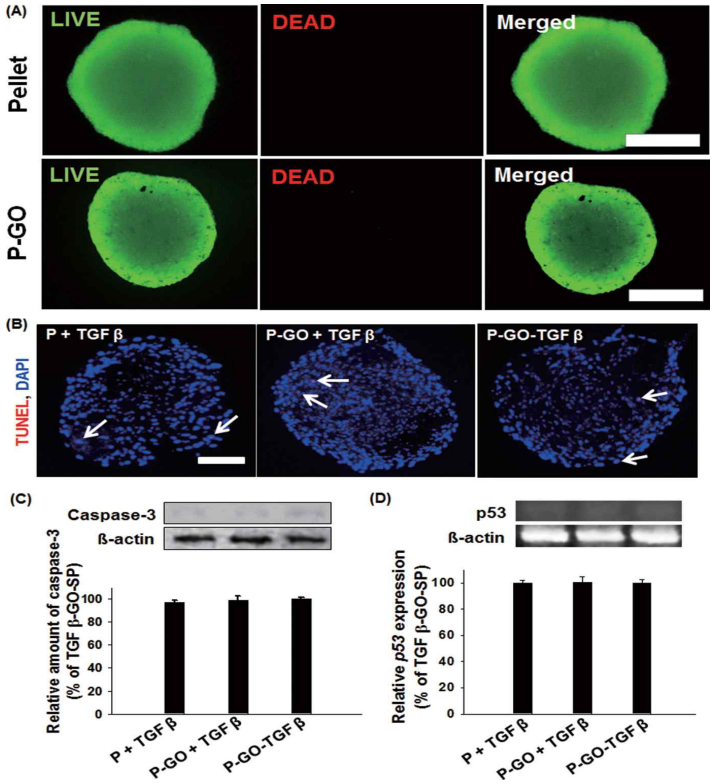

Figure. 4.4. Cytotoxicity of GO sheets evaluated by the viability and apoptotic activity of hASCs in hybrid pellets of GO-hASCs. (A) Viability of hASCs in hASC pellets (Pellet) and hybrid pellets of GO-hASCs (P-GO) evaluated with the FDA-EB assay, which stains live cells green and dead cells red. No red cells were observed in either group. Scale bar indicates 200 μm. (B) The apoptotic activity of hASCs evaluated with the TUNEL assay, which stains apoptotic cells (white arrows) red. Blue (DAPI) indicates nuclei. Scale bar indicates 100 μm. The apoptotic activity of hASCs evaluated by (C) western blotting for caspase-3 expression and (D) RT-PCR of the p53 gene expression (n = 3 for each group). There were no significant differences between any two groups.

3.4. Chondrogenic Differentiation of hASCs

We investigated whether GO sheet incorporation into hASC pellets enhances the chondrogenic differentiation of the hASCs *in vitro*. The chondrogenic differentiation was examined by evaluating the expression of chondrocyte-specific ECMs (aggrecan, glycosaminoglycan, and type II collagen) and the transcription factor (SOX-9). The P-GO-TGF-β group showed a higher deposition of aggrecan compared with the other groups (Figure. 4.5. A). Deposition of type II collagen and glycosaminoglycan was also higher in the P-GO-TGF-β group (Figure. 4.5. B). Western blot analysis also confirmed a higher expression of type II collagen in the P-GO-TGF-β group (Figure. 4.5. C). RT-PCR and real-time PCR results indicated more extensive expression of chondrogenic genes in the P-GO-TGF-β group (Figure. 4.5. D). The P-GO+TGF-β group showed upregulation of SOX-9, a master regulator of chondrogenic differentiation compared with the P+TGF-β group. The expression was further increased in the P-GO-TGF-β group. During endochondral bone development, cells condense and form a cartilage template. Later, the template is terminally converted into bone by mineralization, which is called hypertrophic differentiation.[130] To determine whether the dispersion of FN- and TGF-β3- adsorbed GO sheets in hASC pellets affects hypertrophic differentiation, hypertrophic marker (type X collagen and RUNX2) expression was examined. At late stage of chondrogenic differentiation of ASCs, ASCs could undergo stages of cell hypertrophy and tissue mineralization which leads to bone formation.[131] Since the expression of hypertrophic markers was not different among all groups (Figure. 4.5. E), TGF-β3-adsorbed GO sheets did not promote hypertrophy of the ASCs.[132]

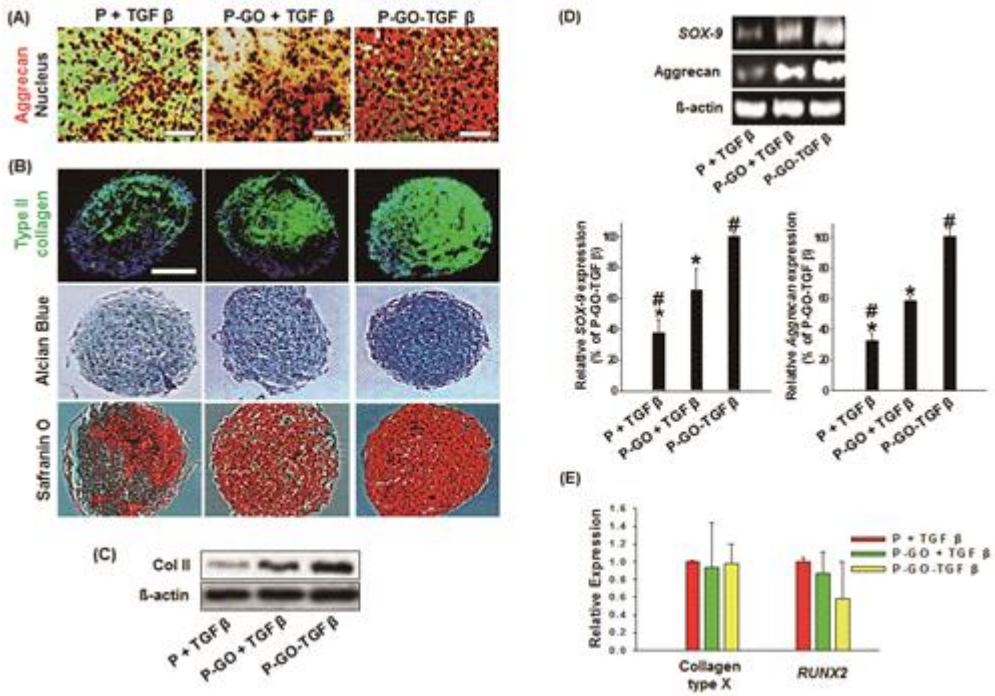

Figure. 4.5. Enhanced chondrogenic differentiation in GO-hASC hybrid pellets at day 14. (A) Immunocytochemical staining for aggrecan. Aggrecan and nuclei were stained brown and black, respectively. Scale bar indicates 30μm. (B) Immunocytochemical staining for typeII collagen (green) and alcian blue and safranin O staining for glycosaminoglycan (blue and red, respectively). In staining for type II collagen, nuclei were counter stained with DAPI (blue). (C) Western blot analysis for type II collagen. (D) RT-PCR (top) and real time-PCR (bottom) analyses for chondrogenic markers. (E) Real-time PCR analysis for hypertrophic markers. Scale bar indicates 100 μm (* p<0.05 versus P-GO-TGF-β, # p<0.05 versus P-GO-TGF-β, n = 3 for each group).

3.5. TGF-β3 Adsorption on GO

To explain the underlying mechanisms of the enhanced chondrogenic differentiation observed in the hybrid pellets, the protein structural stability of TGF-β3 adsorbed on the GO sheets was investigated. It was previously reported that the presence of oxygenated groups on GO can facilitate binding of proteins through electrostatic interactions.[116] In the study, insulin stably interacted with GO and induced adipogenic differentiation of hMSCs. Additionally, the authors showed, by circular dichroism (CD), preserved insulin structure on GO, whereas insulin lost its conformational structure on G. Thus, we hypothesized that GO sheets could stably adsorb TGF-β3 and, by introducing TGF-β3 directly to the cells in the hybrid pellets, could also avoid the diffusional limitation of TGF-β3 to the inner core of the pellets and enhance the chondrogenic differentiation of hASCs. TGF-β3 was stably adsorbed on GO, as evidenced by the negligible release of the protein from the GO sheets over 7 days evaluated with an enzyme-linked immunosorbent assay (ELISA) (Figure. 4.6. A). It was previously reported that hydrophobic and charged side chains of amino acids form π-π and electrostatic interaction with GO and does not dissociate readily. Since TGF-β contains all these amino acids within its sequence, the dissociation could have been negligible.[133] Also, TGF-β receptors are located on the surface of the cells and its interaction with TGF-β3 allows induction of cellular signaling cascade needed for chondrogenic differentiation.[134] Also, when cells interact with TGF-β 3, they initiate molecular pathway to enhance expression of TGF-β3 which are released from the cells and induces chondrogenic differentiation of the neighboring cells.[132] Next, we examined the structural stability of TGF-β3 adsorbed on the GO sheets by comparing the adsorbed structure with the structures of native TGF-β3 and TGF-β3 dissolved in the medium. CD analysis

demonstrated that TGF-β3 closely retained its native structure when adsorbed on GO sheets more than when dissolved in the medium (Figure. 4.6. B). The enhanced structural stability of proteins adsorbed onto GO has been reported previously.[135] Additionally, it was previously reported that proteins are protected from enzymatic attack when bound to GO.[136] These data indicate that GO sheets are capable of adsorbing TGF-β3 and allowing TGF-β3 to retain its structure.

Efficient cellular accessibility of TGF-β3 in the hybrid pellets may also contribute to the enhanced chondrogenic differentiation. TGF-β3 distribution in the pellets was examined with immunostaining for TGF-β3. hASCs are capable of producing their own TGF-β3 under chondrogenic induction conditions.[132] To distinguish the TGF-β3 produced by hASCs from exogenous TGF-β3, mouse-originated TGF-β3 was adsorbed on GO sheets prior to pellet incorporation. The TGF-β3 adsorbed on GO sheets was dispersed throughout the hybrid pellets at 0 and 24 hours of pellet culture (Figure. 4.6. C and D). In contrast, when TGF-β3 was added to the culture medium, diffusion to the pellet inner core was limited, as evidenced by TGF-β3 detection only at the periphery of the pellet at 24 hours of pellet culture (Figure. 4.6. D). It is well known that the diffusional limitation of molecules such oxygen is approximately 150–200 μm in tissues.[123] Diffusional limitation of TGF-β3 in the pellets could limit the chondrogenic differentiation of hASCs in pellet cultures. Therefore, the preserved structure and efficient cellular accessibility of TGF-β3 adsorbed on GO sheets would contribute to the enhanced chondrogenic differentiation of hASCs.

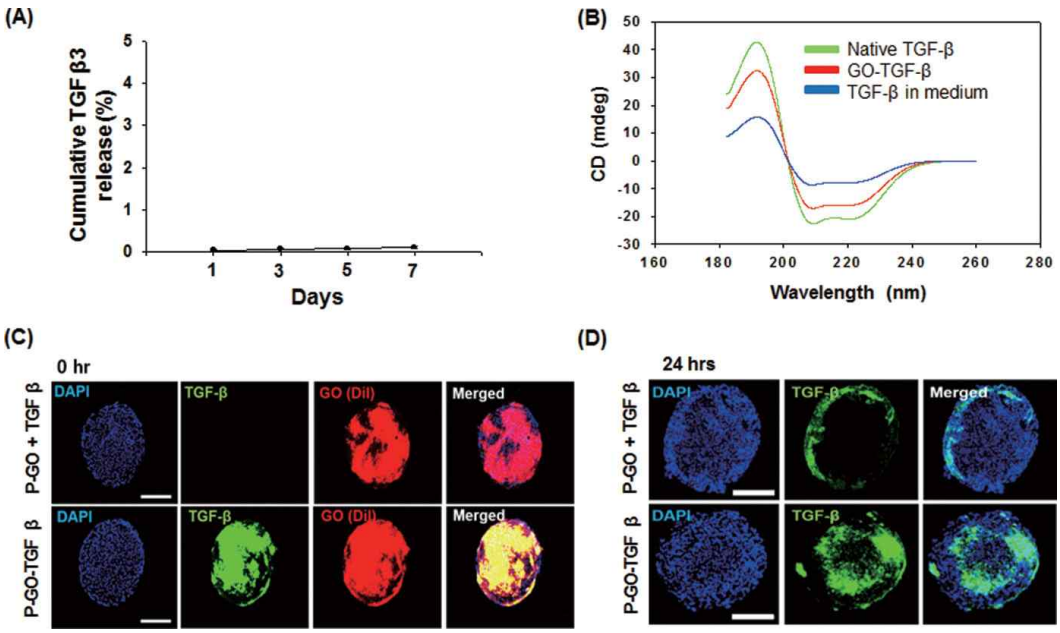

Figure. 4.6. Protein structural stability and cellular accessibility of TGF-β3. (A) Profile of TGF-β3 release from the GO sheets to the medium over 7 days showing stable adsorption on the GO sheets. (B) CD analysis for evaluation of the protein structural stability of TGF-β3 on GO sheets. Immunostaining images and fluorescent images showing the distribution of TGF-β3 (green) adsorbed on GO sheets (red) in the pellet (blue; nuclei) at (C) 0 and (D) 24 hours after pellet formation. Mouse-originated TGF-β3 and an antibody against mouse TGF-β3 were used to distinguish it from the TGF-β3 that might be produced by hASCs. Scale bars indicate 150 μm in (C) and 100 μm in (D).

3.6. Fibronectin Adsorbed on GO

To determine whether GO sheets can serve as a cell-adhesion substrate, cell-adhesion protein (e.g., FN) adsorption on GO sheets was examined. Following incubation of GO sheets in serum-containing medium, we performed energy-dispersive spectroscopy (EDS) and observed sulfur signals that were not present in GO, which confirmed protein adsorption on the GO sheets (Figure. 4.7. A). In addition, EDS mapping showed an even distribution of sulfur on the GO sheets. To determine FN adsorption on the GO sheets, proteins absorbed onto GO was extracted and western blot analysis was performed (Figure. 4.7. B). The results indicate that the proteins adsorbed on the GO sheets include FN. The FN adsorption on GO sheets is likely attributed to the FN interactions with the hydrophobic π domains and hydroxyl groups in the GO sheets. It was previously reported that hydroxyl groups have the strongest FN adsorption compared with amine, carboxyl, and methyl functional groups.[123]

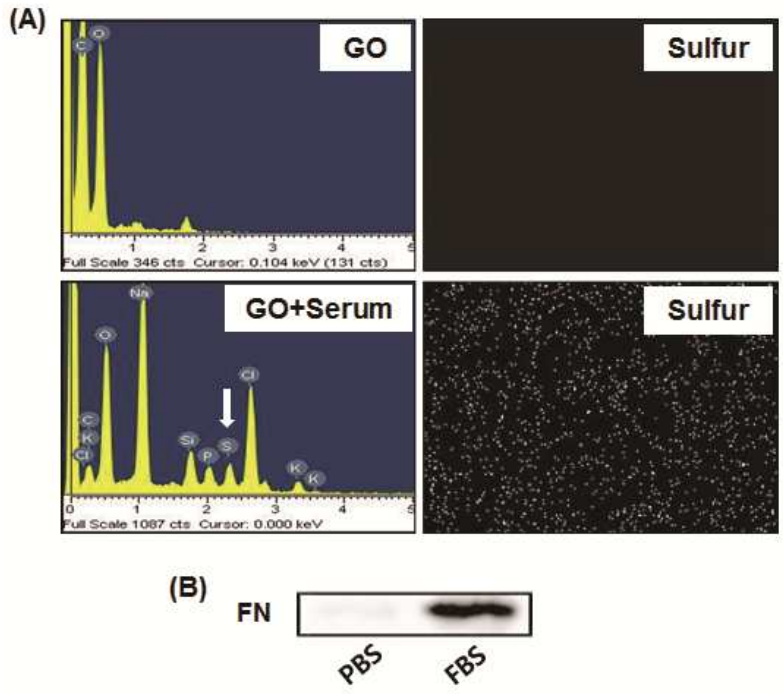

Figure. 4.7. FN adsorption on GO sheets following incubation of GO sheets in culture medium containing 10% (v/v) serum for 4 hours. (A) EDS analysis showing the adsorption of proteins from the serum on GO. The appearance of a sulfuric peak (arrow) and white dots indicate protein adsorption on the GO sheets. (B) Western blot analysis demonstrating the adsorption of FN from serum on the GO sheets.

3.7. Cell Signaling for Chondrogenic Differentiation

The higher protein stability and cellular accessibility of TGF-β3 and the provision of cell-FN interactions in the hASC-GO hybrid pellets promoted cell signaling responsible for chondrogenic differentiation (Figure. 4.8. A). TGF-β initiates chondrogenic differentiation via activation of ERK, JNK, and p38.[137] When TGF-β3 was delivered via GO sheets, the phosphorylation (activation) of all three kinases, ERK, JNK, and p38, increased significantly compared with the other groups (Figure. 4.8. B). This was likely due to the stable and efficient delivery of TGF-β3 using GO in the hybrid pellets. In the P-GO-TGF-β group, the TGF-β3 structure was more stable, and the cellular accessibility of TGF-β3 was not limited inside the pellets (Figure. 4.6. B-D). In contrast, when TGF-β3 was added to the medium, the activation of ERK, JNK, and p38 was significantly decreased compared with the activation when TGF-β3 was delivered via the GO sheets (Figure. 4.8. B). This was likely due to the rapid loss of the stable TGF-β3 protein structure in the medium and the diffusional limitation of TGF-β3 in the pellets (Figure. 4.6. B-D), which would, in turn, limit the chondrogenic differentiation of hASCs.

An additional aspect of the underlying mechanisms of the enhanced chondrogenic differentiation is the interaction between the cells and the FN absorbed on the GO. During early chondrogenesis, FN was reported to enhance cell condensation as well as differentiation of undifferentiated chondroprogenitors.[138] Upon cell interaction with FN, cells initiate chondrogenic differentiation in the region of the cell-FN interaction.[121,122,139] FN plays a functional role in the conversion of mesenchyme to chondroblasts, possibly through internal signaling provided by interaction between the α5β1 integrin and the FN.[140] α5β1 integrin is a FN receptor[141] and the most abundant β

1-containing integrin in fetal cartilage.[142] When FN-adsorbed GO sheets were incorporated to hASC pellets, α5β1 integrin expression was enhanced (Figure. 4.8. C), indicating a cell-FN interaction (Figure. 4.8. C). Thus, by providing FN as a cell-adhesion molecule (Figure. 4.7. B), GO sheets would have contributed to the promotion of chondrogenic differentiation of hASCs.[143]

The enhanced expression of chondrogenic markers in the P-GO+TGF-β group compared with the P+TGF-β group (Figure. 4.5. A-D) was likely due to the adsorption of FN on GO sheets. It is noted that FN was also expressed in the P+TGF-β group at day 1 of culture. This was likely due to the presence of TGF-β3 in the medium because TGF-β can induce FN synthesis.[144] However, the amount of FN was greater in the P-GO-TGF-β group, possibly due to the initial adsorption of FN on the GO (Figure. 4.7.) and the better cellular accessibility of TGF-β3 (Figure. 4.6. D).

GO may be advantageous to G in terms of chondrogenic differentiation of adult stem cells. It was reported that hydroxyl functional groups on GO surfaces have strong affinity for FN, which induces cellular expression of α5β1 integrin that promotes chondrogenic differentiation, compared to other functional groups.[123] In contrast, it was reported that when MSCs adhered on G surfaces, they express focal adhesion kinase (FAK), which promotes osteogenic differentiation.[145] Also, it was reported that insulin proteins denature upon binding to G surface[116], making it unsuitable for protein interaction and delivery in our study.

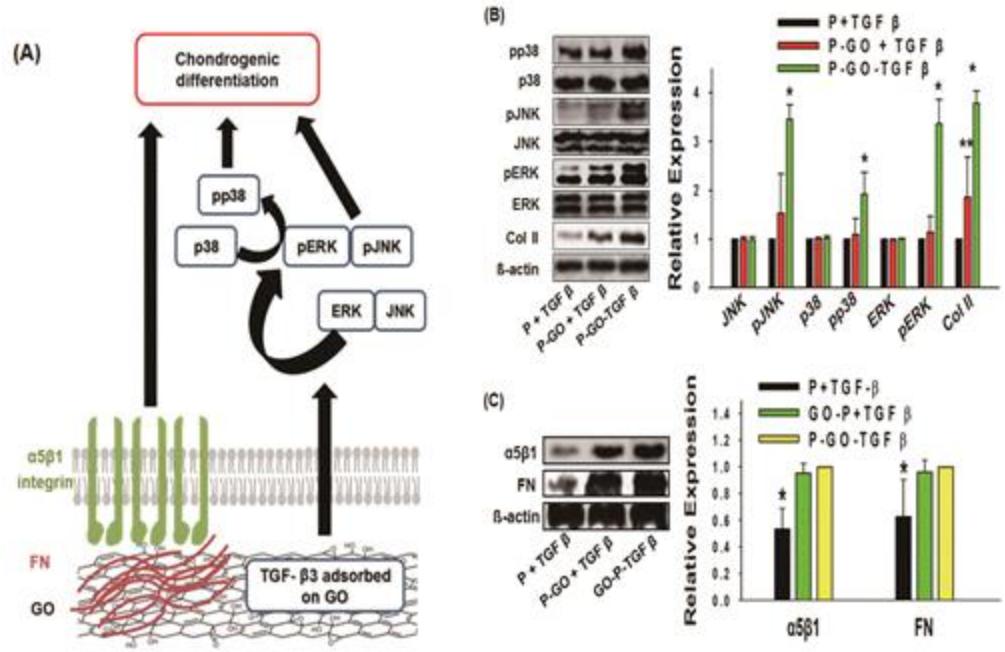

Figure. 4.8. Cell signaling in the enhanced chondrogenic differentiation in the hASC-GO hybrid pellets. (A) A schematic diagram of the underlying mechanisms describing the cell signaling induced by TGF-β3 and FN. (B) Western blot analyses of the qualitative and quantitative expression of activated intracellular signaling molecules related to TGF-β3 signaling. (n = 3 per group, *p<0.05 versus P+TGF-β, #p<0.05 versus P-GO-TGF-β). (C) Western blot analyses of the qualitative and quantitative expression of the α5β 1 integrin, a FN-binding integrin, and FN at day 1 of culture (n = 3 per group, *p<0.05 versus P-GO-TGF-β3, **p<0.05 versus P-GO+TGF-β).

4. Conclusions

This study, for the first time, demonstrates the use of GO to promote chondrogenic differentiation of stem cells. Unlike previous studies using G[116,117,119] or GO[116,118] as a culture substrate in two-dimensional (2D) monolayer culture system for stem cell differentiation, our study used GO as a protein-delivery carrier in a 3D culture system for stem cell differentiation. In conventional pellet culture for chondrogenic differentiation of stem cells, low cell-ECM interaction and the diffusional limitation of TGF-β may limit the chondrogenic differentiation of stem cells. In the present study, FN- and TGF-β -adsorbed GO sheets were incorporated into pellets of hASCs to provide a platform for cell-ECM interaction and to avoid the diffusional limitation of TGF-β, which resulted in significantly enhanced chondrogenic differentiation of hASCs. This study demonstrates that GO can be used to provide cell-adhesion signals and to supply a soluble factor effectively. The use of GO to promote chondrogenic differentiation of stem cells may open a new direction in tissue engineering and regenerative medicine.

Chapter 5

Conclusions

In this study, feasibility of spheroid culture system to induce and enhance chondrogenic differentiation of hASCs were evaluated. In chapter one, the spheroid formation and chondrogenic differentiation of hASCs were induced in large scale by culturing hASCs in three-dimensional suspension bioreactors. *In vitro* chondrogenic differentiation of hASCs was enhanced by spheroid culture compared with monolayer culture. The enhanced chondrogenesis was probably attributable to hypoxia-related cascades and enhanced cell-cell interactions in hASC spheroids. Upon hASCs loading in fibrin gel and transplantation into subcutaneous space of athymic mice for four weeks, the *in vivo* cartilage formation was enhanced by the transplantation of spheroid-cultured hASCs compared with that of monolayer-cultured hASCs. This study shows that spheroid culture may be an effective method for large scale *in vitro* chondrogenic differentiation of hASCs and subsequent *in vivo* cartilage formation. Also, spheroid culture system enhanced cell-cell interaction and induced mild hypoxic condition in the core of the spheroids. Induced hypoxic condition upregulated expression of HIF-1α, which assisted in upregulated expression of TGF-ß3 by phosphrylation of p38.

In chapter two, we show that GO can be utilized as both a cell-adhesion substrate and a growth factor protein-delivery carrier for the chondrogenic differentiation of adult stem cells. GO sheets were utilized to adsorb fibronectin (cell-adhesion protein) and TGF-β3 and were then incorporated in the spheroids. The hybrid spheroids of hASC-GO enhanced the chondrogenic differentiation of hASCs by adding the cell-FN interaction and supplying TGF-β3 effectively.

In conclusion, large scale culture of hASCs by spheroid culture system and feasibility of GO in chondrogenic induction could provide new platform for stem cell culture fo regenerative medicine.

References

1. P. Alan. Articular cartilage repair. *Am. J. Sports Med.* 1992;2:302-24.
2. R.A. Stockwell. Cartilage failure in osteoarthritis: relevance of normal structure and function. *A review.* 1991;4:161.
3. B. Johnstone, M. Alini, M. Cucchiarini, G.R. Dodge, D. Eglin, F. Guilak, et. al. Tissueengineering for articular cartilage repair—the state of the art. *Eur. Cell. Mater.* 2013;25:248.
4. F.W. Bora Jr, G. Miller. Joint physiology, cartilage metabolism, and the etiologyof osteoarthritis. *Hand. Clin.* 1987;3(3):325.
5. H. Muir, The chondrocyte, architect of cartilage. Biomechanics, structure, function and molecular biology of cartilage matrix macromolecules. *Bioessays* 1995;17(12):1039.
6. A. Mobasheri, S. Richardson, R. Mobasheri, M. Shakibaei, J.A. Hoyland. Hypoxia inducible factor-1 and facilitative glucose transporters GLUT1 and GLUT3:putative molecular components of the oxygen and glucose sensing apparatusin articular chondrocytes. *Histol. Histopathol.* 2005;20:1327.
7. E.B. Hunziker. Articular cartilage repair: basic science and clinical progress. A review of the current status and prospects. *Osteoarthritis Cartilage*. 2002;10(6):432.
8. A.I. Caplan M. Elyaderani, Y. Mochizuki, S. Wakitani, V.M. Goldberg. Principles of cartilage repair and regeneration. *Clin. Orthop. Relat. Res*. 1997;342:254.
9. A.I. Caplan, V.M. Goldberg. Principles of tissue engineered regeneration of skeletal tissues. *Clin. Orthop. Relat. Res*. 1999;367 Suppl: S12.
10. E.B. Hunziker L.C. Rosenberg. Repair of partial-thickness defects in articular cartilage: cell recruitment from the synovial membrane. *J. Bone Joint Surg. Am*. 1996;78(5):721.

11. D.W. Jackson, P.A. Lalor, H.M. Aberman, T.M. Simon. Spontaneous repair of full-thickness defects of articular cartilage in a goat model. A preliminary study. *J. Bone Joint Surg. Am*. 2001;83A(1):53.
12. D.W. Jackson, P.A. Lalor, H.M. Aberman, T.M. Simon. Spontaneous repair of full-thickness defects of articular cartilage in a goat model. A preliminary study. *J. Bone Joint Surg. Am*. 2001;83A(1):53.
13. F. Shapiro, S. Koide, M.J. Glimcher. Cell origin and differentiation in the repair of full-thickness defects of articular cartilage. *J. Bone Joint Surg. Am*. 1993;75(4):532.
14. B. Mats. Treatment of deep cartilage defects in the knee with autologous chondrocyte transplantation. *N. Engl. J. Med.* 1994;331:889.
15. M. Cucchiarini, J.K. Venkatesan, M. Ekici, G. Schmitt, h. Madry. Human mesenchymal stem cells overexpressing therapeutic genes: from basic science to clinical applications for articular cartilage repair. *Biomed. Mater. Eng*. 2012;22(4):197.
16. A.I. Caplan. Mesenchymal stem cells. *J. Orthop. Res*. 1991;9(5):641.
17. M.F. Pittenger, A.M. Mackay, S.C. Beck. Multilineage potential of adult human mesenchymal stem cells. *Science*. 1999;284(5411):143.
18. S. Aggarwal, M.F. Pittenger. Human mesenchymal stem cells modulate allogeneic immune cell responses. *Blood*. 2005;105(4):1815.
19. A.I. Caplan, J.E. Dennis. Mesenchymal stem cells as trophic mediators. *J. Cell. Biochem*. 2006;98(5):1076.
20. M.F. Pittensberg, A.M. Mackay, S.C. Beck. Multilineage potential of adult human mesenchymal stem cells. *Science*. 1999;284:143.
21. F. Guilak, B.T. Estes, B.O. Diekman, F.T. Moutos, J.M. Gimble. 2010 nicholas andry award: multipotent adult stem cells from adipose tissue for muscyloskeletal tissue engineering. *Clin. Orthop. Relat. Res.* 2010;468:2530.
22. A. Ucclli, L. A. Uccelli, V. Pistpia. Mesenchymal stem cells in health and

disease. *Nat. Rev. Immunol.* 2008, 8(9), 726.

23. P.B. Harris. Being old: a confrontation group with nursing home residents. *Health Soc. Work*. 1979;4(1):152.
24. P.A. Zuk PA, M. Zhu, P Ashjian. Human adipose tissue is a source of multipotent stem cells. *Mol. Biol. Cell*. 2002;13(12):4279.
25. L. Peng, Z. Jia, X. Yin. Comparative analysis of mesenchymal stem cells from bone marrow, cartilage, and adipose tissue. *Stem Cells Dev*. 2008;17(4):761.
26. J.J. Minguell, A. Erices, P. Conget. Minireview: mesenchymal stem cells, *Exp. Biol. Med.* 226 (2001) 507.
27. E.B. Hunziker, I.M. Driesang, E.A. Morris. Chondrogenesis in cartilage repair is induced by members of the transforming gorwth factor-beta superfamily. *Curr. Orthopae. Prac.* 2001;391:s171.
28. S. Ichinose, M. Tagami, T. Muneta, I. Sekiya.. Morphological exmination during in vitro cartilage formation by human mesenchymal stem cells. *Cell Tissue Res.* 2005, 322, 217.
29. W. Hunter, Of the structure and disease of articulating cartilages. 1743. *Clin. Orthop. Relat. Res*. 1995;317:3.
30. B.L. Clair, A.R. Johnson, T. Howard. Cartilage repair: current and emerging options in treatment. *Foot Ankle Spec*. 2009;2(4):179.
31. T.A. Ahmed, M.T. Hincke. Strategies for articular cartilage lesion repair and functional restoration. *Tissue Eng. Part B Rev*. 2010;16(3):305.
32. E.B. Hunziker, Articular cartilage repair: basic science and clinical progress. A review of the current status and prospects. *Osteoarthritis Cartilage*. 2002;10(6):432.
33. C. Chung C, J.A. Burdick. Engineering cartilage tissue. *Adv. Drug Deliv. Rev*. 2008;60(2):243.
34. G.J. van Osch, M. Brittberg, J.E. Dennis et. al. Cartilage repair: past and

future lessons for regenerative medicine. *J. Cell. Mol. Med*. 2009;13(5): 792.

35. S. Ehnert, M. Glanemann, A. Schmitt et. al. The possible use of stem cells in regenerative medicine: dream or reality? *Langenbecks Arch. Surg*. 2009;394(6):985.
36. N.P. Cohen, R.J. Foster, V.C. Mow. Composition and dynamics of articular cartilage: structure, function, and maintaining healthy state. *J. Orthop. Sports Phys. Ther.* 1998;28:203.
37. J.A. Buckwalter, Articular cartilage. *AAOS Inst. Course Lect.* 1983;32:349.
38. J.A. Buckwalter, H.J. Mankin. Articular cartilage: tissue design and chondrocyte}matrix interactions. *AAOS Inst. Course Lect.* 1998;47:477
39. J. Malda, W. ten Hoope, W. Schuurman, G.I. van Osch, P.R. van Weeren, W.J. Dhert. Localization of the potential zonal marker clusterin in native cartilage and in tissue-engineered constructs. *Tissue Eng. Part A*. 2010;16(3):897.
40. S.D. Waldman, M.D. Grynpas, R.M. Pilliar, R.A. Kandel. The use of specific chondrocyte populations to modulate the properties of tissue-engineered cartilage. *J. Orthop. Res*. 2003;21(1):132.
41. W. Schuurman, D. Gawlitta, T.J. Klein, et al. Zonal chondrocyte subpopulations reacquire zone-specific characteristics during *in vitro* redifferentiation. *Am. J. Sports Med*. 2009;37 Suppl 1:S97–S104.
42. M. Brittberg, A. Lindahl, A. Nilsson, C. Ohlsson, O. Isaksson, L. Peterson. Treatment of deep cartilage defects in the knee with autologous chondrocyte transplantation. *N. Engl. J. Med*. 1994;331(14):889.
43. H. Vasiliadis, C. Salanti, A. Georgoulis, A. Lindahl, L. Peterson. Assessment of clinical outcomes 10–20 years after autologous chondrocyte implantation. *Osteoarthritis Cartilage*. Epub 2010 May 5.
44. L. Peterson, H.S. Vasiliadis, M. Brittberg, A. Lindahl. Autologous chondrocyte implantation: a long-term follow-up. *Am. J. Sports Med*. 2010;38(6):1117.

45. G. Knutsen, L. Engebretsen, T.C. Ludvigsen, et. al. Autologous chondrocyte implantation compared with microfracture in the knee. A randomized trial. *J. Bone Joint Surg. Am*. 2004;86-A(3):455.
46. H.S. Vasiliadis, J. Wasiak, G. Salanti. Autologous chondrocyte implantation for the treatment of cartilage lesions of the knee: a systematic review of randomized studies. *Knee Surg. Sports Traumatol. Arthrosc*. 2010;18(12);1645.
47. A. Bedi, B.T. Feeley, R.J. Williams. Management of articular cartilage defects of the knee. *J Bone Joint Surg. Am*. 2010;92(4):994.
48. J.R. Steadman, K.K. Briggs, J.J. Rodrigo, M.S. Kocher, T.J. Gill, W.G. Rodkey. Outcomes of microfracture for traumatic chondral defects of the knee: average 11-year follow-up. *Arthroscopy*. 2003;19(5): 477.
49. H.S. Vasiliadis, J. Wasiak, G. Salanti. Autologous chondrocyte implantation for the treatment of cartilage lesions of the knee: a systematic review of randomized studies. *Knee Surg. Sports Traumatol. Arthrosc*. 2010;18(12):1645.
50. B. Dozin, M. Malpeli, R. Cancedda. et. al. Comparative evaluation of autologous chondrocyte implantation and mosaicplasty: a multicentered randomized clinical trial. *Clin. J. Sport Med*. 2005;15(4):220.
51. R. Gudas, E. Stankevicius, E. Monastyreckiene, D. Pranys, R.J. Kalesinskas. Osteochondral autologous transplantation versus microfracture for the treatment of articular cartilage defects in the knee joint in athletes. *Knee Surg. Sports Traumatol. Arthrosc*. 2006;14(9):834.
52. L. Zheng, H.S. Fan, J. Sun, et al. Chondrogenic differentiation of mesenchymal stem cells induced by collagen-based hydrogel: an in vivo study. *J. Biomed. Mater. Res. A*. 2010;93(2):783.
53. M.W. Kessler, D.A. Grande. Tissue engineering and cartilage. *Organogenesis*. 2008;4(1):28.

54. L. Meinel, S. Hofmann, V. Karageorgiou, et al. Engineering cartilage-like tissue using human mesenchymal stem cells and silk protein scaffolds. *Biotechnol. Bioeng*. 2004;88(3):379.

55. J. Xu, W. Wang, M. Ludeman, et al. Chondrogenic differentiation of human mesenchymal stem cells in three-dimensional alginate gels. *Tissue Eng. Part A*. 2008;14(5):667.

56. T. Re'em, O. Tsur-Gang, S. Cohen. The effect of immobilized RGD peptide in macroporous alginate scaffolds on TGF-beta1-induced chondrogenesis of human mesenchymal stem cells. *Biomaterials*. 2010; 31(26):6746.

57. S. Wakitani, T. Goto, S.J. Pineda, et al. Mesenchymal cell-based repair of large, full-thickness defects of articular cartilage. *J. Bone Joint Surg. Am*. 1994;76(4):579.

58. S. Wakitani, T. Okabe, S. Horibe, et al. Safety of autologous bone marrowderived mesenchymal stem cell transplantation for cartilage repair in 41 patients with 45 joints followed for up to 11 years and 5 months. *J. Tissue Eng. Regen. Med*. 2011;5(2);146.

59. S. Wakitani, M. Nawata, K. Tensho, T. Okabe, H. Machida, H. Ohgushi. Repair of articular cartilage defects in the patello-femoral joint with autologous bone marrow mesenchymal cell transplantation: three case reports involving nine defects in five knees. *J. Tissue Eng. Regen. Med*. 2007;1(1):74.

60. S. Wakitani, T. Mitsuoka, N. Nakamura, Y. Toritsuka, Y. Nakamura, S. Horibe. Autologous bone marrow stromal cell transplantation for repair of full-thickness articular cartilage defects in human patellae: two case reports. *Cell Transplant*. 2004;13(5):595.

61. S. Wakitani, K. Imoto, T. Yamamoto, M. Saito, N. Murata, M. Yoneda. Human autologous culture expanded bone marrow mesenchymal cell transplantation for repair of cartilage defects in osteoarthritic knees.

Osteoarthritis Cartilage. 2002;10(3):199.

62. S.N. Jung, J.W. Rhie, H. Kwon, et al. *In vivo* cartilage formation using chondrogenic-differentiated human adipose-derived mesenchymal stem cells mixed with fibrin glue. *J. Craniofac. Surg*. 2010;21(2):468.
63. F. Hildner, S. Wolbank, H. Redl, M. van Griensven, A. Peterbauer. How chondrogenic are human umbilical cord matrix cells? A comparison to adipose-derived stem cells. *J. Tissue Eng. Regen. Med*. 2009;4(3): 242.
64. R.B. Jakobsen, A. Shahdadfar, F.P. Reinholt, J.E. Brinchmann. Chondrogenesis in a hyaluronic acid scaffold: comparison between chondrocytes and MSC from bone marrow and adipose tissue. *Knee Surg. Sports Traumatol. Arthrosc*. 2010;18(10);1407.
65. J.L. Dragoo, G. Carlson, F. McCormick, et al. Healing full-thickness cartilage defects using adipose-derived stem cells. *Tissue Eng*. 2007;13(7): 1615.
66. K.H. Prodie. Mesenchymal stem cells and cartilage *in situ* regeneration. *J. Intern. Med*. 2009;266(4):390.
67. K. Mithoefer, et. al. Chondral resurfacing of articular cartilage defects in the knee with the microfracture technique. Surgical technique. *J. Bone Joint Srg. Am.* 2006;88:294.
68. D.D. Frisbie. A comparative study of articular cartilage thichness in the stifle of animal species used in human preclinical studies compared to articular cartilage thickness in the human knee. *Vet. Comp. Orthop Traumatol.* 2006;19(3):142.
69. D.D. Frisbie. Early events in cartilage repair after subchondral bone microfracture. *Clin. Orthop. Relat. Res*. 2003;407:215.
70. D.B. Saris, et. al. Treatment of symptomatic cartilage defects of the knee: characterized chondrocyte implantation results in better clinical outcome at 36 months in a randomized trial compared to microfracture. *Am. J. Sports Med.* 2009;37:10S.

71. M. Brittberg, et. al. Treatment of deep cartilage defects in the knee with autologous chondrocyte transplantation. *N. Engl. J. Med.* 1994;331:889.

72. M. Brittberg, A. Lindahl, A. Nilsson, et al. Treatment of osteochondritis dissecans of the knee with autologous chondrocyte transplantation: results at 2–10 years. *J. Bone. Joint Surg. Am.* 2003;85A(suppl 2):17.

73. L. Peterson, T. Minas, M. Brittberg, et. al.. Two to 9 year outcome after autologous chondrocyte transplantation of the knee. *Clin. Orthop. Relat. Res.* 2000;374:212.

74. C.R. Gooding, A prospective, randomised study comparing two techniques of autologous chondrocyte implantation for osteochondral defects in the knee: Periosteum covered versus type I/III collagen covered. *Knee* 2006;13:203.

75. A.H. Gomoll, C. Probst, J. Farr, B.J. Cole, T.Minas. Use of a type I/III bilayer collagen membrane decreases reoperation rates for symptomatic hypertrophy after autologous chondrocyte implantation. *Am. J. Sports Med.* 2009;37 (Suppl. 1):20S.

76. M. Marcacci, Articular cartilage engineering with Hyalograft C: 3 year clinical results. *Clin. Orthop. Relat. Res.* 2005;435:96.

77. E.M. Darling, K.A. Athanasiou. Rapid phenotypic changes in passaged articular chondrocyte subpopulations. *J. Orthop. Res.* 2005;23:425.

78. I. Martinez, J. Elvenes, R. Olsen, K. Bertheussen, O. Johansen. Redifferentiation of *in vitro* expanded adult articular chondrocytes by combining the hanging-drop cultivation method with hypoxic environment. *Cell Transplant.* 2008;17: 987.

79. E.A. Makris. Hypoxia-induced collagen crosslinking as a mechanism for enhancing mechanical propeties of engineered articular cartilage. *Osteoarthritis Cartilage*. 2013;21:634.

80. J.M. Patrascu. Repair of a post-traumatic cartilage defect with a cell-free polymer-based cartilage implant: a follow-up at two years by MRI and

histological review. *J. Bone Joint Surg. Br.* 2010; 92:1160.

81. S. Patel. Treatment with platelet rich plasma is more effective than placebo for knee osteoarthritis: a prospective, double-blind, randomized trial. *Am. J. Sports Med*. 2013;41:356.
82. W.D. Stanish, et. al. Novel scaffold-based BST-CarGel treatment results in superior carilage repair compared with microfracture in a randomized controlled trial. *J. Bone Joint Surg. Am*. 2013;95: 1640.
83. N.J. Gunja. Effective TGF-beta1 and hydrostatic pressure on meniscus cell-seeded scaffolds. *Biomaterials*. 2009;30:565.
84. U. Meyer, et. al. Cartilage defect regeneration by *ex vivo* engineering autologous microtissue-prelininary results. *In Vivo*. 2012;26: 251.
85. C.R. Lee, A.J. Grodzinsky, H.P. Hsu, S.D. Martin, M. Spector. Effects of harvest and selected cartilage repair procedures on the physical and biochemical properties of articular cartilage in the canine knee. *J. Orthop. Res.* 2000;18:790.
86. D.J. Prockop. Marrow stromal cells as stem cells for nonhematopoietic tissues. *Science* 1997:276:71.
87. A.M. Rodriguez, C. Elabd, E.Z. Amri, G. Ailhaud, C. Dani. The human adipose tissue is a source of multipotent stem cells. *Biochimie* 2005;87:25.
88. L. Casteilla, V. Planat-Benard, B. Cousin, J.S. Silvestre, P. Laharrague, G. Charrière, L. Penicaud. Plasticity of adipose tissue: A promising therapeutic avenue in the treatment of cardiovascular and blood diseases. *Arch. Mal. Coeur. Vaiss.* 2005;98:922.
89. M. Oedayrajsingh-Varma, S. van Ham, M. Knippenberg, M.N. Helder, J. Klein-Nulend, T.E. Schouten, M.J Ritt, F.J. van Milligen. Adipose tissue-derived mesencymal stem cell yield and growth characteristics are affected by the tissue-harvesting procedure. *Cytotherapy* 2006;8:166.
90. G.I. Im, Y.W. Shin, K.B. Lee. Do adipose tissue-derived mesenchymal stem

cells have the same osteogenic and chondrogenic potential as bone marrow-derived cells? *Osteoarthritis cartilage.* 2005;13:845.

91. H. Afizah, Z. Yang, J.H. Hui, H.W. Ouyang, E.H. Lee. A comparison between the chondrogenic potential of human bone marrow stem cells (BMSCs) and adipose-derived stem cells (ASCs) taken from the same donor. *Tissue Eng.* 2007;13:659.
92. A. Technau, K. Froelich, R. Hagen, N. Kleinsasser. Adipose tissue-derived stem cells show both immunogenic and immunosuppressive properties after chondrogenic differentiation. *Cytotherapy* 2011;13:310.
93. A. Winter, S. Breit, D. Parsch, K. Benz, E. Steck, H. Hauner, R.M. Weber, V. Ewerbeck, W. Richter. Cartilage-like gene expression in differentiated human stem cell spheroids: a comparison of bone marrow-dericed and adipose tissue-derived strolmal cells. *Arthritis Rheum.* 2003;48: 418.
94. D. Bosnakovski, M. Mizuno, G. Kim, S. Takagi, M. Okumura, T. Fujinaga. Chondrogenic differentiation of bovine bone marrow mesenchymal stem cells (MSCs) in different hydrogels: influence of collagen type II extracellular matrix on MSC chondrogenesis. *Biotechnol. Bioeng.* 2006;93:1152.
95. C. Chung, J.A. Burdick. Influence of three-dimensional hyaluronic acid microenvironments on mesenchymal stem cell chondrogenesis. *Tissue Eng. Part A* 2009;15: 243.
96. J.H. Ryu, M.S. Kim, G.M. Lee, C.Y, Choi, B.S. Kim. The enhancement of recombinant protein production by polymer nanospheres in cell suspension culture. *Biomaterials* 2005;26:2173.
97. S.H. Bhang, S.W. Cho, W.G. La, T.J. Lee, H.S. Yang, A.Y. Sun, S.H. Baek, J.W. Rhie, B.S. Kim. Angiogenesis in ischemic tissue produced by spheroid grafting of human adipose-derived stromal cells. *Biomaterials* 2011;32:2734.
98. M. Kanichai, D. Ferguson, P.J. Prendergast, V.A. Campbell. Hypoxia promotes chondrogenesis in rat mesenchymal stem cells: a role for AKT and

hypoxia-inducible factor (HIF)-1α. *J. Cell Physiol.* 2008;216:708.

99. L. Peterson, T. Minas, M. Brittberg, A. Lindahi. Treatment of osteochondritis dissecans of the knee with autologous chondrocyte transplantation: results at two to ten years. *J. Bone Joint Surg. Am.* 2003;85-A:17.
100. S. Ichinose, M. Tagami, T. Muneta, I. Sekiya. Morphological examination during *in vitro* cartilage formation by human mesenchymal stem cells. *Cell. Tissue Res.* 2005;322;217.
101. S.A. Oberlender, R.S. Tuan. Expression and functional involvement of N-cadherin in embryonic limb chondrogenesis. *Development* 1994;120:177.
102. A.M. DeLise, R.S. Tuan. Analysis of N-cadherin function in limb mesenchymal chondrogenesis *in vitro*. *Dev. Dyn.* 2002;225:195.
103. D. Shweiki, M. Neeman, E. Keshet. Induction of vascular endothelial growth factor expression by hypoxia and by glucose deficiency in multicell spheroids: implication for tumor angiogenesis. *Proc. Natl. Acad. Sci. USA* 1995;92:768.
104. R. Amarilio, S.V. Viukov, A. Sharir, I. Eshkar-Oren, R.S. Johnson, E. Zelzer. HIF-1α regulation of Sox9 us necessary to maintain differentiation of hypoxic prechondrogenic cells during early skeletogenesis. *Development* 2007;134:3917.
105. C.L. Murphy, J.M. Polak. Control of human articular chondrocyte differentiation by reduced oxygen tension. *J. Cell. Physiol.* 2004;199:451.
106. I. Sekiya, K. Tsuji, P. Koopman, H. Watanabe, Y. Yamada, K. Shinomiya, A. Nifuji, M. Noda. SOX9 enhances aggrecan gene promoter/enhancer activity and is up-regulated by retinoic acid in a cartilage-derived cell line, TC6. *J. Biol. Chem* 2000;275:10738.
107. L.A. McMahon. et. al. A comparison of the involvement of p38, ERK1/2 and PI3K in growth factor-induced chondrogenic differentiation of mesenchymal stem cells. *Biochem. Biophys. Res. Commun.* 2008;368:990.

108. C.D. Oh, S.H. Chang, Y.M. Yoon, S.J. Lee, Y.S. Lee, S.S. Kang, J.S. Chun. Opposing role of mitogen-activated protein kinase subtypes, erk-1/2 and p38, in the regulation of chondrogenesis of mesenchymes. *J. Biol. Chem.* 2000;275:5613.

109. J.C. Robins, N. Akeno, A. Mukherjee, R.R. Dalal, B.J. Aronow. Koopman P., and Clemens T.L. Hypoxia induces chondrocyte-specific gene expression in mesenchymal cells in association with transcriptional activation of SOX9. *Bone* 2005;37:313.

110. G. Liu, W. Ding, J. Neiman, K.M. Mulder. Requirement of Smad3 and CREB-1 in mediating transforming growth factor-β (TGF-β) induction of TGF-β3 secretion. *J. Biol. Chem.* 2006;281:29479.

111. Z. Zhang, Q. Lu, J. Zhao, H. Huang, Z. Shen, Z. Zhang. Enhanced Chemotherapy Efficacy by Sequential Delivery of siRNA and Anticancer Drugs Using PEI-Grafted Graphene Oxide, *Small* 2011;7:460.

112. K.P. Liu. et. al. Green and facile synthesis of highly biocompatible graphene nanosheets and its application for cellular imaging and drug delivery. *J. Mater. Chem.* 2011;21:12034.

113. O. Akhavan, E. Ghaderi, H. Emamy,. Nontoxic concentrations of PEGylated graphene nanoribbons for selective cancer cell imaging and photothermal therapy. *J. Mater. Chem*. 2012;22:20626.

114. K. Yang, J. Wan, S. Zjang, B. Tian, Y. Zhang, Z. Yiu. The influence of surface chemistry and size of nanoscale graphene oxide on photothermal therapy of cancer using ultra-low laser power. *Biomaterials* 2012;33:2206.

115. W.C. Lee, C.H.Y.X. Lim, H. Shi, A.L. Tang, Y. Wang, C.T. Lim, K.P Loh. Origin of enhanced stem cell growth and differentiation on graphene and graphene oxide. *ACS Nano* 2011;5:7334.

116. S.Y. Park, J. Park, S.H. Sim, M.G. Sung, K.S. Kim, B.H. Hong, S. Hong, Enhanced differentiation of human neural stem cells into neurons on

graphene, *Adv. Mater.* 2011;23:H263.

117. S.H. Ku, C.B. Park, Myoblast differentiation on graphene oxide. *Biomaterials* 2013;34:2017.

118. T.R. Nayak, H. Anderse, C. S. Makam, C. Khaw, S. Bae, X. Xu, P.-L. Ee, J.-H. Ahn, B.H. Hong, G. Pastorin, B. Ozyilmaz. Graphene for controlled and accelerated osteogenic differentiation of human mesenchymal stem cells. *ACS Nano* 2011;5:4670.

119. H. Afizah, Z. Yang, J.H. Hui, H. W. Ouyang, E.H. Lee, A comparison between the chondrogenic potential of human bone marrow stem cells (BMSCs) and adipose-derived stem cells (ADSCs) taken from the same donors. *Tissue Eng.* 2007;13:659.

120. D.A. Frenz, N.S. Jaikaria, S.A. Newman, The mechanism of precartilage mesenchymal condensation: a major role for interaction of the cell surface with the amino-terminal heparin-binding domain of fibronectin. *Dev. Biol.* 1989;136:97.

121. B.K. Hall, et. al. All for one and one for all: condensations and the initiation of skeletal development. *Bioessays* 2000;22:138.

122. G. Mehta, A.Y. Hsiao, M. Ingram, G.D. Luker, S. Takayama, Opportunities and challenges for use of tumor spheroids as models to test drug delivery and efficacy. *J. Control Release* 2012;16:192.

123. B.G. Keselowsky, D.M. Collard, A.J. Garcia, Surface chemistry modulates fibronectin conformation and directs integrin binding and specificity to control cell adhesion. *J. Biomed Mater. Res.* A. 2003;66:247.

124. D.C. Marcano, D.V. Kosynkin, J.M. Berlin, A. Sinitskii, G. Sun, A. Slesarev, L.B. Alemany, W. Lu, J.M. Tour, Improved synthesis of graphene oxide. *ACS Nano* 2010;4:4806.

125. A.C. Ferrari, J.C. Meyer, V. Scardaci, C. Casiraghi, M. Lazzeri, F. Mauri, S. Piscanec, D. Jiang, K.S. Novoselov, S. Roth, K. Geim,Raman spectrum of

graphene and graphene layers. *Phys. Rev. Lett.* 2006;97:187401.

126. S. Stankovich, D.A. Dikin, R.D. Piner, K.A. Kohlhaas, A. Kleinhammes, Y. Jia, Y. Wu, S.T. Nguyen, R.S. Ruoff. Synthesis of graphene-based nanosheets via chemical reduction of exfoliated graphite oxide. *Carbon* 2007;45:1558.
127. M. Sinoforoglu, B. Gur, M. Arik, Y. Onganer, K. Meral. Graphene oxide sheets as a template for dye assembly:graphene oxide sheets induce H-aggregates of pyronin (Y) dye. *RSC Adv.* 2013;3:11832.
128. O. Akhavan, E. Ghaderi, A. Akhavan, Size-dependent genotoxicity of graphene nanoplatelets in human stem cells. *Biomaterial* 2012;33:8017.
129. E.J. Marckie, L. Ahmed, K.-S. Tatarczuch, C.M. Mirams. Endochondral ossification: how cartilage is converted into bone in the developing skeleton. *Int. J. Biochem. Cell Biol.* 2008;40:46.
130. K. Pelttari, A. Winter, E. Stech, K. Goetzke, T. Hennig, B.G. Ochs, T. Aigner, W. Richter. Premature induction of hypertrophy during *in vitro* chondrogenesis of human mesenchymal stem cells correlates with calcification and vascular invasion after ectopic transplantation in SCID mice. *Arthritis Rheum.* 2006;54:3254.
131. H.H. Yoon, S.H. Bhang, J.-Y. Shin, J.H. Shin, B.-S. Kim Enhanced cartilage formation via three-dimensional cell engineering of human adipose-derived stem cells. *Tissue Eng.* 2012;18:1949.
132. M. Zhang, et. al. Interaction of peptides with graphene oxide and its application for real-time monitoring of protease activity. *Chem. Commun.* 2011;47:2399.
133. M. Motoyama, M. Deie, A. Kanaya, M. Nishimori, A. Miyamoto, S. Yanada, N. Adachi, M. Ochi. *In vitro* cartilage formation using TGF-beta-immobilized magnetic beads and mesenchymal stem cell-magnetic bead complexes under magnetic field conditions. *J. Biomed. Mater. Res. A.* 2010;92:196.

134. W.G. La, S. Park, H.H. Yoon, G.-J. Jeong, T.-J. Lee, S.H. Bhang, J.Y. Han, K. Char, B.-S. Kim, Delivery of a therapeutic protein for bone regeneration from a substrate coated with graphene oxide. *Small* 2013;9(23):4051.

135. H. Shen, M. Liu, H. He, L. Zhang, J. Huang, Y. Chong, J. Dai, Z. Zhang,. PEGylated graphene oxide-mediated protein delivery for cell function regulation. *ACS Appl. Mater. Interfaces* 2012;4:6317.

136. R. Tuli, S. Tuli, S. Nandi, X. Huang, P.A. Manner, W.J. Hozack, K.G. Danielson, D.J. Hall, R.S. Tuan, Transforming growth factor-beta-mediated chondrogenesis of human mesenchymal progenitor cells involves N-cadherin and mitogen-activated protein kinase and Wnt signaling cross-talk. *J. Biol. Chem.* 2003;278:41227.

137. S. Ghosh, M. Laha, S. Mondal, S. Sengupta, D.L. Kaplan. *In vitro* model of mesenchymal condensation during chondrogenic development. *Biomaterials* 2009;30:6530.

138. R.B. Widelitz, T.X. Jiang, et. al. Adhesion molecules in skeletogenesis: II. Neural cell adhesion molecules mediate precartilaginous mesenchymal condensations and enhance chondrogenesis. *J. Cell. Physiol.* 1993;156:399.

139. A.M. Delise, L. Fischer, R.S. Tuan, Cellular interactions and signaling in cartilage development. *Osteoarthritis Cartilage* 2000;8:309.

140.. M.A. Lan, C.A. Gersbach, K.E. Michael, B.G. Keselowsky, A. Myoblast proliferation and differentiation on fibronectin-coated self assembled monolayers presenting different surface chemistries. *Biomaterials* 2005;26:4523.

141. G. Hausler, M. Hemereich, S. Marlovits, M. Egerbacher, Integrins and extracellular matrix proteins in the human childhood and adolescent growth plate. *Calcif. Tissue Int.* 2002;71:212.

142. P. Singh, J. E. Schwarzbauer, Fibronectin and stem cell differentiation - lessons from chondrogenesis. *J. Cell Sci*. 2012;125:3703.

143. B.S. Weston, et. al. CTGF mediates TGF-beta-induced fibronectin matrix deposition by upregulating active alpha5beta1 integrin in human mesangial cells, *J. Am. Nephrol.* 2003;14:601.

144. M. Kalbacova, A. Broz, J. Kong, M. Kalbac,. Graphene substrates promote adherence of human osteoblasts and mesenchymal stromal cel. *Carbon*, 2010;48:4323.

145. M.S. Hummer, R.E. Offeman, Preparation of graphitic oxide. *J. Am. Chem. Soc.* 1958;80:1339.

146. B.G. Choi, Y.S. Huh, Y.C. Park, D.W. Hung, W.H. Hong, H. Park, Enhanced transport properties in polymer electrolyte composite membranes with graphene oxide sheets. *Carbon* 2012;50:5395.

147. S.H. Bhang, S. Lee, J.Y. Shin, T.J. Lee, B.S. Kim, Transplantation of cord blood mesenchymal stem cells as spheroids enhances vascularization. *Tissue Eng. Part A*. 2012;18:2138.

국문초록

스페로이드 배양기법을 사용한 지방유래 줄기세포의 연골분화 증진

손상된 초자연골의 경우 혈관이 없기 때문에 자기재생이 어렵다는 문제점이 있다. 초자연골의 재생을 돕기 위하여 현재 자가연골 이식술이 실행되어지고 있지만 이 방법은 이식을 진행하기 위하여 많은 양의 연골세포를 필요로 하며, 이를 위하여 체외에서 연골세포를 증식시키게 된다. 이 치료법은 여러 번의 수술을 통하여 이루어지며 수술을 통하여 진행된 연골세포의 채취가 이미 발생한 연골의 손상을 더욱 악화 시킬 수 있으며, 또한 이식을 위해 체외에서 연골세포를 증식시킬 때 역분화의 발생이 문제가 되기 때문에 골수 또는 지방 같은 성체조직에서 분획 가능한 성체줄기세포를 이용한 치료적 접근이 시도되고 있다. 이중 지방유례 줄기세포는 반복적인 접근과 비교적 손쉬운 분획법으로 연골재생에 이용될 수 있는 매력적인 세포주로 생각되어지기에 이번 실험에서 사용하고자 하였다.

이전의 성체줄기세포를 이용한 연골분화는 세포들을 하나의 거대한 덩어리인 펠렛으로 만들어 성장인자, 덱사메타손, 그리고 ascorbate-2-phsphate의 첨가로 시도되어 졌지만, 영양분 확산의 저하 및 펠렛 중심부에 부여되는 강한 저산소 조건에 의하여 세포의 사멸이 일어날 수 있다는 문제점을 갖고 있어 연골분화에 부적합한 배양법으로 사료된다. 이번 연구에서는 이러한 문제점을 극복하고자 세포들을 소규모 펠렛인 “스페로이드”로 만들고 이들 통해 연골분화를 유도함으로서 앞에서 언급한 부적절한 조건들을 극복하고자 하였다.

제 3장에서는 스페로이드 배양기법을 도입하여 연골분화에 적합한 저산소 조건을 유도하고, 또한 세포간의 상호작용을 증진하여 줄기세포의 연골 분화능을 증진할 수 있다는 가설 하에 실험을 진행하였다. 이 두 가지 조건들을 이미 연골분화에 긍정적인 영향을 미친다고 알려져 있다. 기존에 스페로이드를 만든는 방법은

일정량의 세포를 방울로 만들어 매달아 놓는 'hanging-drop' 기법으로 진행되었다. 이번 연구에서는 hanging-drop이 아닌 스피너 플라스크를 사용하여 더욱 쉽고 간편하게 스페로이드를 형성하였다. 이러하게 형성된 스페로이드는 스피너 플라스크에서 14일간 배양한 후, 일반 배양과 비교하여 연골분화의 정도를 분석하였다. 연골분화의 증진은 저산소 조건과 세포간의 증진으로 설명될 수 있을 것이며, 이와 같이 분화된 스페로이드를 fibrin gel과 섞어 소동물의 피하에 접종하였을 경우 증진된 연골 형성능을 확인할 수 있었다.

제 4장에서는 그래핀 옥사이드의 응용이 연골분화의 증진이 미치는 영향을 관찰하였다. 우리는 그래핀 옥사이드가 갖고 있는 작용기들이 fibronectin과 같은 세포 부착물과 반응 가능하며, 또한 성장인자들과 안정하게 반응하여 줄기세포의 연골분화 증진에 기여할 것이라 가설하였으며, 이를 바탕으로 앞서 언급한 스페로이드 배양기법에 그래핀 옥사이드를 적용하여 그래핀 옥사이드가 연골분화에 미치는 영향을 분자 화학적으로 확인하였다. 그래핀 옥사이드는 π 부분과 카르복실 및 하이드록실 작용기를 가지고 있다. π 전자 구름은 파이브로넥틴의 소수성 중심 구조 및 성장인자와 작용할 수 있다. Hydroxyl기의 경우 fibronectin의 구조를 안정화한다는 연구가 발표되어 있으며, 안정한 fibronectin의 제공으로 인테그린의 발편을 증진시켜 연골분화를 촉진하도록 하였다. 또한, 정전기적 작용으로 성장인자를 그래핀 옥사이드의 작용기들과 반응시켜 동일한 결과를 얻고자 하였다. 이와 같은 기작을 이용하고자 그래핀 옥사이드를 스페로이드 형성에 참여시켰으며, 스피너 플라스크 배양 후 연골분화의 촉진을 확인하였다.

주요어: 지방유례 줄기세포, 연골분화, 스페로이드, 그래핀 옥사이드, 조직공학

학번: 2010- 21003